Painlevé monodromy manifolds, decorated character varieties, and cluster algebras

Chekhov, Leonid; Mazzocco, Marta; Rubtsov, Vladimir

DOI:
10.1093/imrn/rnw219

Document Version
Peer reviewed version

Citation for published version (Harvard):
Chekhov, L, Mazzocco, M & Rubtsov, V 2017, 'Painlevé monodromy manifolds, decorated character varieties, and cluster algebras', *International Mathematics Research Notices*, vol. 2017, no. 24, pp. 7639–7691. https://doi.org/10.1093/imrn/rnw219

Chekhov, L., Mazzocco, M. and Rubtsov, V. (0000) "Painlevé monodromy manifolds, decorated character varieties and cluster algebras," International Mathematics Research Notices, Vol. 0000, Article ID rnn000, 31 pages.
doi:10.1093/imrn/rnn000

Painlevé monodromy manifolds, decorated character varieties and cluster algebras

Leonid Chekhov[1], Marta Mazzocco[2], Vladimir Rubtsov[3]

[1]Steklov Mathematical Institute, Moscow, Russia. QGM, Århus University, Denmark. Email: chekhov@mi.ras.ru. [2]Department of Mathematical Sciences, Loughborough University, UK. Email: m.mazzocco@lboro.ac.uk. [3]Mathematics Department, University of Angers, France. Email: volodya@tonton.univ-angers.fr.

Correspondence to be sent to: m.mazzocco@lboro.ac.uk

In this paper we introduce the concept of decorated character variety for the Riemann surfaces arising in the theory of the Painlevé differential equations. Since all Painlevé differential equations (apart from the sixth one) exhibit Stokes phenomenon, we show that it is natural to consider Riemann spheres with holes and bordered cusps on such holes. The decorated character variety is considered here as complexification of the bordered cusped Teichmüller space introduced in arXiv:1509.07044. We show that the decorated character variety of a Riemann sphere with s holes and $n \geq 1$ bordered cusps is a Poisson manifold of dimension $3s + 2n - 6$ and we explicitly compute the Poisson brackets which are naturally of cluster type. We also show how to obtain the confluence procedure of the Painlevé differential equations in geometric terms.

1 Introduction

The Painlevé differential equations describe monodromy preserving deformations of auxiliary linear systems of two first order ODEs on the punctured Riemann sphere. The monodromy and Stokes matrices of this linear system are encoded in the so-called *monodromy manifolds*. For example in the case of the sixth Painlevé equation, that describes the isomonodromic deformations of a flat SL_2–connection on $\mathbb{P}^1$ with four regular singularities, the monodromy manifold is realised as the Fricke-Klein affine cubic surface [25]. Many mathematicians have obtained similar formulae for all other Painlevé equations, and recently Saito and van der Put [36] have provided a unified approach in which they showed the existence of ten families of affine cubic surfaces that can be realised as monodromy manifolds for the Painlevé differential equations. One of the aims of our paper is to give a geometric interpretation of this classification and to prove that the confluence procedure of the Painlevé differential equations corresponds to a new type of surgery on Riemann surfaces called *chewing-gum* [11].

It is well known that the sixth Painlevé monodromy manifold is the $SL_2(\mathbb{C})$ character variety of a 4 holed Riemann sphere. The real slice of this character variety is the decorated Teichmüller space of a 4 holed Riemann sphere, and can be combinatorially described by a fat-graph and shear coordinates. By complexifying the shear coordinates, flat coordinates for the character variety of a 4 holed Riemann sphere were found in [10]. For the other Painlevé equations, the interpretation of their monodromy manifolds as "character varieties" of a Riemann sphere with boundary is still an extremely difficult problem due to the fact that the linear problems associated to the other Painlevé equations exhibit Stokes phenomenon. This implies that some of the boundaries have *bordered cusps* on them [11]. Being on the boundary, these bordered cusps escape the usual notion of character variety leading to the necessity of introducing a decoration.

In this paper we present a decoration which truly encodes the geometry of each cusped boundary. On the real slice of our decorated character variety, this decoration corresponds to choosing some horocycles to associate a λ-length to each bordered cusp.* This geometric description allows us to introduce flat coordinates in the corresponding *bordered cusped Teichmüller space* (see [11] for the definition of this notion) and, by complexification, on the decorated character variety.

This leads us to define explicitly a set of coordinates on the decorated character variety of the Riemann spheres with bordered cusps which arise in the theory of the Painlevé differential equations and to compute the

Received 1 December 2015; Revised 27 June 2016; Accepted 14 September 2016

*We use the term bordered cusp meaning a vertex of an ideal triangle in the Poincaré metric in order to distinguish it from standard cusps (without borders) associated to punctures on a Riemann surface.

Poisson brackets in these coordinates. Such Poisson brackets coincide with the cluster algebra Poisson structure as predicted in [11].

We note that another approach to this problem was developed in [5] where the definition of wild character variety was proposed following a construction by Gaiotto, Moore and Neitzke [19] which consisted in introducing spurious punctures at the points of intersection between the Stokes lines and some fixed circles around each irregular singularity. This description does not seem compatible with the confluence procedure of the Painlevé equations nor with the case of isomonodromic deformations in which all singularities are non-simple poles (such as the one associated to $PIII^{D_8}$), which is one of our motivations to propose a new approach.

We show that, if we exclude PVI, we have nine possible Riemann surfaces with bordered cusps, for which we define the decorated character variety. We show that in each case there is a specific Poisson sub-algebra that is the coordinate ring of an affine variety - the monodromy manifold of the given Painlevé differential equation. These monodromy manifolds can all be described by affine cubic surfaces in $\mathbb{C}^3$ defined by the zero locus of the corresponding polynomials in $\mathbb{C}[x_1, x_2, x_3]$ given in Table 1, where $\omega_1, \dots, \omega_4$ are some constants related to the parameters appearing in the corresponding Painlevé equation as described in Section 2.

P-eqs	Polynomials
PVI	$x_1x_2x_3 + x_1^2 + x_2^2 + x_3^2 + \omega_1 x_1 + \omega_2 x_2 + \omega_3 x_3 + \omega_4$
PV	$x_1x_2x_3 + x_1^2 + x_2^2 + \omega_1 x_1 + \omega_2 x_2 + \omega_3 x_3 + 1 + \omega_3^2 - \frac{\omega_3(\omega_2+\omega_1\omega_3)(\omega_1+\omega_2\omega_3)}{(\omega_3^2-1)^2}$
PV_{deg}	$x_1x_2x_3 + x_1^2 + x_2^2 + \omega_1 x_1 + \omega_2 x_2 + \omega_1 - 1$
PIV	$x_1x_2x_3 + x_1^2 + \omega_1 x_1 + \omega_2(x_2 + x_3) + \omega_2(1 + \omega_1 - \omega_2)$
$PIII^{D_6}$	$x_1x_2x_3 + x_1^2 + x_2^2 + \omega_1 x_1 + \omega_2 x_2 + \omega_1 - 1$
$PIII^{D_7}$	$x_1x_2x_3 + x_1^2 + x_2^2 + \omega_1 x_1 - x_2$
$PIII^{D_8}$	$x_1x_2x_3 + x_1^2 + x_2^2 - x_2$
PII^{JM}	$x_1x_2x_3 - x_1 + \omega_2 x_2 - x_3 - \omega_2 + 1$
PII^{FN}	$x_1x_2x_3 + x_1^2 + \omega_1 x_1 - x_2 - 1$
PI	$x_1x_2x_3 - x_1 - x_2 + 1$

Table 1.

Note that in Table 1, we distinguish ten different monodromy manifolds, the $PIII^{D_6}$, $PIII^{D_7}$ and $PIII^{D_8}$ correspond to the three different cases of the third Painlevé equation according to Sakai's classification [37], and the two monodromy manifolds PII^{FN} and PII^{JM} associated to the same second Painlevé equation correspond to the two different isomonodromy problems found by Flaschka–Newell [16] and Jimbo–Miwa [26] respectively.

Our methodology consists in reproducing the famous confluence scheme for the Painlevé equations:

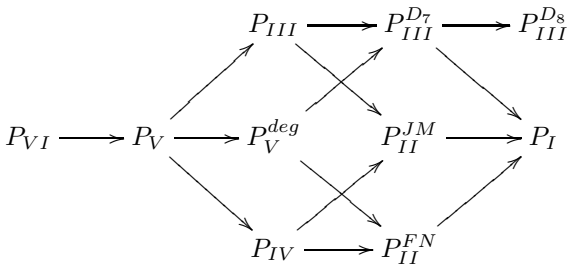

in terms of the following two *chewing-gum operations* on the underlying Riemann sphere:

- *Hole–hooking:* hook two holes together and stretch to infinity by keeping the area between them finite (see Fig. 1).
- *Cusps removal:* pull two cusps on the same hole away by tearing off an ideal triangle (see Fig. 2).

As shown by the first two authors in [11], these two operations correspond to certain asymptotics in the shear coordinates and perimeters. We will deal with such asymptotics in Section 5. The confluence process on the underlying Riemann spheres with cusped boundaries is described in Fig. 3.

In our work, cluster algebras appear naturally when describing the bordered cusped Teichmüller space of each Riemann sphere with bordered cusps. Indeed, as shown in [11], when bordered cusps arise, it is possible to introduce a *generalized lamination* on the Riemann surface consisting only of geodesics which start and terminate at the cusps. The geodesic length functions (well defined by fixing horocycles at each cusp) in this lamination are the coordinates in the bordered cusped Teichmüller space, while the decoration itself is given by the choice of

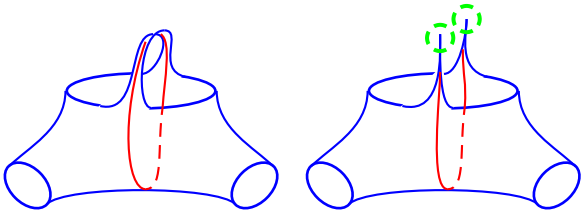

Fig. 1. The process of confluence of two holes on the Riemann sphere with four holes: as a result we obtain a Riemann sphere with one less hole, but with two new cusps on the boundary of this hole. The geodesic line which was initially closed becomes infinite, therefore two horocycles (the dashed circles) must be introduced in order to measure its length.

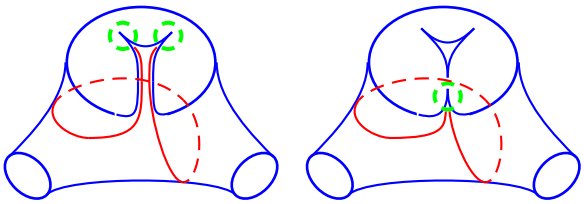

Fig. 2. The process of breaking up a Riemann surface with boundary cusps: by grabbing together two cusps and pulling we tear apart an ideal triangle.

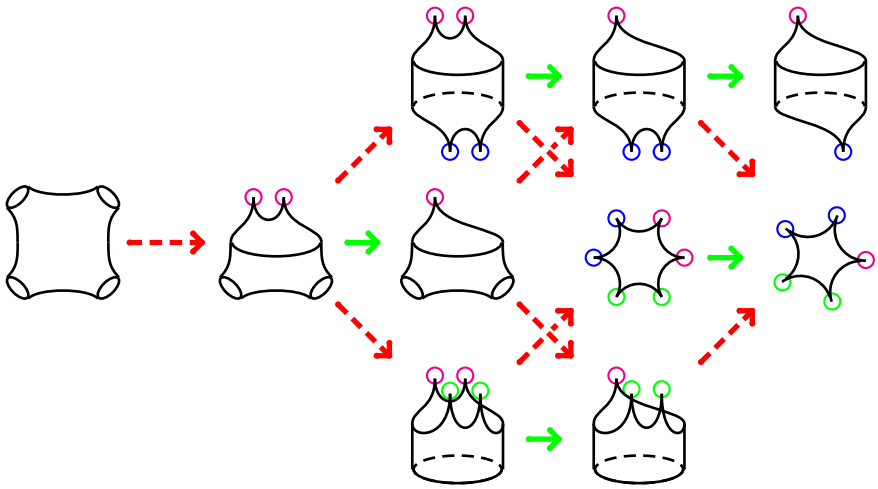

Fig. 3. The table of confluences of Riemann surfaces from the Painlevé perspective. The long dashed arrows correspond to chewing-gum moves, the short solid ones to cusp removal.

horocycles. In the Poisson structure given by the Goldman bracket, these coordinates satisfy the cluster algebra Poisson bracket. This is due to the fact that the geodesics in the lamination do not intersect in the interior of the Riemann sphere, but come together asymptotically in the bordered cusps.

We also study the corresponding cluster mutations and show that in the case of a Riemann sphere with four holes they correspond to the procedure of analytic continuation for solutions to the sixth Painlevé equation, thus showing that this procedure of analytic continuation satisfies the Laurent phenomenon. For the other Painlevé equations, the cluster algebra mutations correspond to the action of the Mapping Class Group on the cusped lamination.

Since our decorated character variety is the complexification of the bordered cusped Teichmüller space, by complexifying the coordinates of the latter given by the generalized laminations we obtain coordinates on the decorated character varieties. We show that in the case of the Painlevé differential equations, the decorated character variety is a Poisson manifold of dimension $3s + 2n - 6$, where s is the number of holes and $n \geq 1$ is the number of cusps. We show that in each case the decorated character variety admits a special Poisson sub–manifold defined by the set of functions which Poisson commute with the frozen cluster variables. This sub–manifold is defined as a cubic surface $\mathcal{M}_\phi := \mathrm{Spec}(\mathbb{C}[x_1, x_2, x_3]/\langle \phi = 0 \rangle)$, where ϕ is one of the polynomials

in Table 1, with the natural Poisson bracket defined by:

$$\{x_1, x_2\} = \frac{\partial \phi}{\partial x_3}, \quad \{x_2, x_3\} = \frac{\partial \phi}{\partial x_1}, \quad \{x_3, x_1\} = \frac{\partial \phi}{\partial x_2}. \tag{1.1}$$

Interestingly, when confluencing the decorated character varieties, the short solid arrows in Fig. 3 must be *reversed,* while the long dashed arrows remain pointing in the same direction. In this way we obtain a graph explaining the inclusions of the Poisson algebras on each character variety:

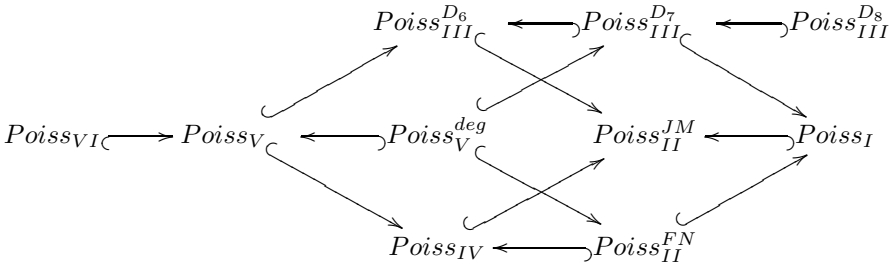

Therefore the most general Poisson algebra is the one associated to a Riemann sphere with one hole and 6 bordered cusps (the one associated to PII^{JM}), and all the other Poisson algebras can be obtained as Poisson sub-algebras of this one.†

We note that in [32] the monodromy manifolds arising in the case of the Painlevé differential equations were quantized to obtain the spherical sub-algebras of certain confluent versions of the Cherednik algebra of type $\check{C}_1 C_1$. The role of cluster algebras in the Cherednik algebra setting will be investigated further in subsequent publications.

This paper is organized as follows: in Section 2, we recall the link between the parameters $\omega_1, \dots, \omega_4$ and the Painlevé parameters α, β, γ and δ in each Painlevé equation and discuss the natural Poisson bracket (1.1) on each cubic. In Section 3, we remind some important notions on the combinatorial description on the bordered cusped Teichmüller space. In Section 4, we introduce the notion of decorated character variety. In Section 5, we present the flat coordinates for each cubic and describe the laminations and the corresponding cluster algebra structure. In Section 6, we explain the generalized cluster algebra structure appearing in the case of PVI, PV, $PIII^{D_6}$ and PIV. In the Appendices we discuss the geometric meaning of the *Katz invariant* and the interpretation of each Painlevé monodromy manifold as versal deformation of a certain singularity.

2 The Painlevé monodromy manifolds and their Poisson structure

According to [36], the monodromy manifolds $\mathcal{M}^{(d)}$ have all the form

$$x_1 x_2 x_3 + \epsilon_1^{(d)} x_1^2 + \epsilon_2^{(d)} x_2^2 + \epsilon_3^{(d)} x_3^2 + \omega_1^{(d)} x_1 + \omega_2^{(d)} x_2 + \omega_3^{(d)} x_3 + \omega_4^{(d)} = 0, \tag{2.2}$$

where d is an index running on the list of the Painlevé cubics PVI, PV, PV_{deg}, PIV, $PIII^{D_6}, PIII^{D_7}$, $PIII^{D_8}, PII^{JM}, PII^{FN}, PI$ and the parameters $\epsilon_i^{(d)}$, $\omega_i^{(d)}$, $i = 1, 2, 3$ are given by:

$$\epsilon_1^{(d)} = \begin{cases} 1 & \text{for } d = PVI, PV, PIII^{D_6}, PV_{deg}, PIII^{D_7}, PIII^{D_8}, PIV, PII^{FN}, \\ 0 & \text{for } d = PII^{JM}, PI, \end{cases}$$

$$\epsilon_2^{(d)} = \begin{cases} 1 & \text{for } d = PVI, PV, PIII^{D_6}, PV_{deg}, PIII^{D_7}, PIII^{D_8} \\ 0 & \text{for } d = PIV, PII^{FN}, PII^{JM}, PI, \end{cases}$$

$$\epsilon_3^{(d)} = \begin{cases} 1 & \text{for } d = PVI, \\ 0 & \text{for } d = PV, PIII^{D_6}, PV_{deg}, PIII^{D_7}, PIII^{D_8}, PIV, PII^{FN}, PII^{JM}, PI. \end{cases}$$

while

$$\begin{aligned} &\omega_1^{(d)} = -G_1^{(d)} G_\infty^{(d)} - \epsilon_1^{(d)} G_2^{(d)} G_3^{(d)}, \quad \omega_2^{(d)} = -G_2^{(d)} G_\infty^{(d)} - \epsilon_2^{(d)} G_1^{(d)} G_3^{(d)}, \\ &\omega_3^{(d)} = -G_3^{(d)} G_\infty^{(d)} - \epsilon_3^{(d)} G_1^{(d)} G_2^{(d)}, \\ &\omega_4^{(d)} = \epsilon_2^{(d)} \epsilon_3^{(d)} \left(G_1^{(d)}\right)^2 + \epsilon_1^{(d)} \epsilon_3^{(d)} \left(G_2^{(d)}\right)^2 + \epsilon_1^{(d)} \epsilon_2^{(d)} \left(G_3^{(d)}\right)^2 + \left(G_\infty^{(d)}\right)^2 + \\ &\qquad + G_1^{(d)} G_2^{(d)} G_3^{(d)} G_\infty^{(d)} - 4 \epsilon_1^{(d)} \epsilon_2^{(d)} \epsilon_3^{(d)}, \end{aligned} \tag{2.3}$$

†We are grateful to the referee for asking to clarify this point.

where $G_1^{(d)}, G_2^{(d)}, G_3^{(d)}, G_\infty^{(d)}$ are some constants related to the parameters appearing in the Painlevé equations as follows:

$$G_1^{(d)} = \begin{cases} 2\cos\pi\theta_0 & d = PVI, PV, PIII^{D_6}, PV_{deg}, PIV, PII^{FN} \\ 1 & d = PIII^{D_8}, PII^{JM}, PI \\ \infty & d = PIII^{D_7}, \\ 0 & d = PIII^{D_8}, \end{cases}$$

$$G_2^{(d)} = \begin{cases} 2\cos\pi\theta_1 & d = PVI, PV, \\ 2\cos\pi\theta_\infty & d = PIII^{D_6}, PV_{deg}, PIV, \\ e^{i\pi\theta_0} & d = PII^{JM} \\ 1 & d = PIII^{D_8}, PII^{FN}\, PI \\ \infty & d = PIII^{D_7}, PIII^{D_8}, \end{cases}$$

$$G_3^{(d)} = \begin{cases} 2\cos\pi\theta_t & d = PVI, \\ 2\cos\pi\theta_\infty & d = PV, PIV \\ 1 & d = PII^{JM}, \\ 0 & d = PIII^{D_6}, PV_{deg}, PIII^{D_7}, PIII^{D_8}, PII^{FN}, PI \end{cases} \tag{2.4}$$

$$G_\infty^{(d)} = \begin{cases} 2\cos\pi\theta_\infty & d = PVI, PIV \\ 1 & d = PV, PV_{deg}, D_8, PII^{JM}, PII^{FN}, PI \\ e^{i\pi\theta_0} & d = PIII^{D_6} \\ 0 & d = PIII^{D_7}, PIII^{D_8}. \end{cases}$$

where the parameters $\theta_0, \theta_1, \theta_t, \theta_\infty$ are related to the Painlevé equations parameters in the usual way [26]. Note that for $PIII^{D_7}$ the parameters G_1 and G_2 tend to infinity - we take this limit in such a way that $\omega_1 = -G_1 G_\infty$ and $\omega_2 = -G_2 G_\infty$ are not zero, while $\omega_4 = 0$. Similarly for $PIII^{D_8}$.

Remark 2.1. Observe that in the article [36] the cubic corresponding to the Flaschka–Newell isomonodromic problem [16] is in the form $x_1x_2x_3 + x_1 - x_2 + x_3 + 2\cos\pi\theta_0 = 0$. This can be obtained from our cubic $x_1x_2x_3 + x_1^2 + \omega_1 x_1 - x_2 + 1$ by the following diffeomorphism (away from $x_2x_3 = 0$):

$$x_1 \to -sx_1, \qquad x_2 \to \frac{1}{s}x_2, \quad x_3 \to \frac{s^2x_1^2 - \frac{1+x_1x_2}{s}x_3}{x_1x_2},$$

where $s = 2\cos\pi\theta_0$. The reason to choose the cubic in the form PII^{FN} will be clear in Section 5. □

Remark 2.2. Note that the $PIII^{D_7}$, $PIII^{D_8}$ and PI cubics have different signs in [36], which can both be obtained by a trivial rescaling of the variables x_1, x_2, x_3. □

2.1 Natural Poisson bracket on the monodromy manifold

We would like to address here some natural facts that arise when comparing the various descriptions of family of affine cubics surfaces with 3 lines at infinity (2.2).

First of all, the projective completion of the family of cubics 2.2 with $\epsilon_i^{(d)} \neq 0$ for all $i = 1, 2, 3$ has singular points only in the finite part of the surface and if any of $\epsilon_i^{(d)}, i = 1, 2, 3$ vanish, then $\mathcal{M}^{(d)}$ is singular at infinity with singular points in homogeneous coordinates $X_i = 1$ and $X_j = 0, j \neq i$ ([33]). Here $x_i = \frac{X_i}{X_0}$.

One can consider this family of cubics as a variety $\mathcal{S} = \{(\bar{x}, \bar{\omega}) \in \mathbb{C}^3 \times \Omega) : S(\bar{x}, \bar{\omega}) = 0\}$ where $\bar{x} = (x_1, x_2, x_3)$, $\bar{\omega} = (\omega_1, \omega_2, \omega_3, \omega_4)$ and the "$\bar{x}-$forgetful" projection $\pi : \mathcal{S} \to \Omega$ such that $\pi(\bar{x}, \bar{\omega}) = \bar{\omega}$. This projection defines a family of affine cubics with generically non–singular fibres $\pi^{-1}(\bar{\omega})$ (we will discuss the nature of these singularities in Appendix B).

The cubic surface $S_{\bar{\omega}}$ has a volume form $\vartheta_{\bar{\omega}}$ given by the Poincaré residue formulae:

$$\vartheta_{\bar{\omega}} = \frac{dx_1 \wedge dx_2}{(\partial\phi)/(\partial x_3)} = \frac{dx_2 \wedge dx_3}{(\partial\phi)/(\partial x_1)} = \frac{dx_3 \wedge dx_1}{(\partial\phi)/(\partial x_2)}, \tag{2.5}$$

where ϕ is given in Table 1.

The volume form is a holomorphic 2-form on the non-singular part of $S_{\bar{\omega}}$ and it has singularities along the singular locus. This form defines the Poisson brackets on the surface in the usual way as:

$$\{x_1, x_2\}_{\bar{\omega}} = \frac{\partial\phi}{\partial x_3}, \quad \{x_2, x_3\}_{\bar{\omega}} = \frac{\partial\phi}{\partial x_1}, \quad \{x_3, x_1\}_{\bar{\omega}} = \frac{\partial\phi}{\partial x_2}. \tag{2.6}$$

By computing the derivative of ϕ we obtain the volume form (2.5) as

$$\vartheta_{\bar\omega}=\frac{dx_i\wedge dx_j}{(\partial\phi)/(\partial x_k)}=\frac{dx_i\wedge dx_j}{(x_ix_j+2\epsilon_i^dx_k+\omega_i^d)}, \tag{2.7}$$

where $(i,j,k)=(1,2,3)$ up to cyclic permutation.

In a special case of PVI , i.e. the $\widetilde{D}_4$ cubic with parameters $\omega_i=0$ for $i=1,2,3$ and $\omega_4=-4$, there is an isomorphism $\pi:\mathbb{C}^*\times\mathbb{C}^*/\eta\to\phi$: [7]

$$\pi(u,v)\to(x_1,x_2,x_3)=(-u-1/u,-v-1/v,-uv-1/uv), \tag{2.8}$$

where η is the involution of $\mathbb{C}^*\times\mathbb{C}^*$ given by $u\to 1/u,\quad v\to 1/v$. The log-canonical 2-form $\bar\vartheta=\frac{du\wedge dv}{uv}$ defines a symplectic structure on $\mathbb{C}^*\times\mathbb{C}^*$ which is invariant with respect the involution η and therefore defines a symplectic structure on the non-singular part of the cubic surface $S_{\bar\omega}$ for $\omega_i=0$ for $i=1,2,3$ and $\omega_4=-4$.

The relation between the log-canonical 2-form $\bar\vartheta=\frac{du\wedge dv}{uv}$ and the Poisson brackets on the surface $S_{\bar\omega}$ can be extended to all values of the parameters $\bar\omega$ and for all the Painlevé cubics as we shall show in this paper. In fact the flat coordinates that we will introduce in Section 5 are such that their exponentials satisfy the log-canonical Poisson bracket.

Remark 2.3. The cubic $\mathcal{M}^{(PVI)}$ appears in many different contexts outside of the Painlevé theory. For example, it was studied in Oblomkov' s work (see [33]) in relation to Cherednik algebras and M. Gross, P. Hacking and S.Keel (see Example 5.12 of [22]) claim that the family 2.2 can be "uniformized" by some analogues of theta-functions related to toric mirror data on log-Calabi-Yau surfaces. More precisely, the projectivisation Y of 2.2 with the cubic divisor $\Delta: X_1X_2X_3=0$ is an example of so called *Looijenga pair* and $Y\setminus\Delta$ is a log-symplectic Calabi-Yau variety with the holomorphic 2-form 2.5. We shall quantize this log-Calabi-Yau variety in the subsequent paper [13]. □

3 Combinatorial description of the bordered cusped Teichmüller space

Let us start with the standard case, i.e. when no cusps are present. According to Fock [17] [18], the fat graph associated to a Riemann surface $\Sigma_{g,s}$ of genus g and with s holes is a connected three–valent graph drawn without self-intersections on $\Sigma_{g,s}$ with a prescribed cyclic ordering of labelled edges entering each vertex; it must be a maximal graph in the sense that its complement on the Riemann surface is a set of disjoint polygons (faces), each polygon containing exactly one hole (and becoming simply connected after gluing this hole). In the case of a Riemann sphere $\Sigma_{0,4}$ with 4 holes, the fat–graph is represented in Fig. 4.

The geodesic length functions, which are traces of hyperbolic elements in the Fuchsian group $\Delta_{g,s}$ such that

$$\Sigma_{g,s}\sim\mathbb{H}/\Delta_{g,s}$$

are obtained by decomposing each hyperbolic matrix $\gamma\in\Delta_{g,s}$ into a product of the so–called *right, left and edge matrices:*

$$R:=\begin{pmatrix}1&1\\-1&0\end{pmatrix},\qquad L:=\begin{pmatrix}0&1\\-1&1\end{pmatrix},\qquad X_{s_i}:=\begin{pmatrix}0&-\exp\left(\frac{s_i}{2}\right)\\ \exp\left(-\frac{s_i}{2}\right)&0\end{pmatrix},$$

where s_i is the shear coordinate associated to the i-th edge in the fat graph.

In [11] the notion of fat-graph was extended to allow cusps. Here we present this definition adapted to the special cases dealt in the current paper:

Definition 3.1. We call *cusped fat graph* (a graph with the prescribed cyclic ordering of edges entering each vertex) $\mathcal{G}_{g,s,n}$ a *spine of the Riemann surface* $\Sigma_{g,s,n}$ with g handles, s holes and $n>0$ decorated bordered cusps if

(a) this graph can be embedded without self-intersections in $\Sigma_{g,s,n}$;
(b) all vertices of $\mathcal{G}_{g,s,n}$ are three-valent except exactly n one-valent vertices (endpoints of the open edges), which are placed at the corresponding bordered cusps;
(c) upon cutting along all *nonopen* edges of $\mathcal{G}_{g,s,n}$ the Riemann surface $\Sigma_{g,s,n}$ splits into s polygons each containing exactly one hole and being simply connected upon contracting this hole.

□

Definition 3.2. We call geometric *cusped geodesic lamination* (CGL) on a bordered cusped Riemann surface a set of nondirected curves up to a homotopic equivalence such that

(a) these curves are either closed curves (γ) or *arcs* ($\mathfrak{a}$) that start and terminate at bordered cusps (which can be the same cusp);
(b) these curves have no (self)intersections inside the Riemann surface (but can be incident to the same bordered cusp);
(c) these curves are not empty loops or empty loops starting and terminating at the same cusp.

□

In the case of arcs, the geodesic length functions are now replaced by the signed geodesic lengths of the parts of arcs contained between two horocycles decorating the corresponding bordered cusps; the sign is negative when these horocycles intersect.

Combinatorially speaking this corresponds to calculating the lengths of such arcs by associating to each arc a matrix in $SL_2(\mathbb{R})$ in the same way as before, i.e. by taking products of left, right and edge matrices, but then by taking the trace of such product of matrices *multiplied by the cusp matrix:* $K = \begin{pmatrix} 0 & 0 \\ -1 & 0 \end{pmatrix}$ *at the right hand side of the whole expression.* For example the arc b in Fig. 6 has length l_b such that

$$\exp\left(\frac{l_b}{2}\right) = \mathrm{Tr}\left(X(k_1)RX(s_3)RX(s_2)RX(p_2)RX(s_2)LX(s_3)LX(k_1)K\right).$$

Note that in all fat graphs in this paper we distinguish the shear coordinates s_1, s_2, s_3 which correspond to the edges in the central T shaped part of the graph and the shear coordinates $k_1, \ldots, k_6$ correspond to the cusps which arise when breaking holes.

In [11] it is proved that for every cusped fat-graph with the additional property that the polygons containing holes with no cusps are monogons, there exists a complete cusped geodesic lamination which consists only of arcs and simple loops around the un-cusped holes. Loosely speaking, this means that all lengths of any closed geodesic or of any arc in the Riemann surface is a Laurent polynomial of the lengths of the elements in the lamination.

The Poisson brackets between lengths of arcs and closed geodesics can be computed by using the Weil–Petersson bracket, which in shear coordinates becomes [8, 9]

$$\left\{f(\mathbf{Z}), g(\mathbf{Z})\right\} = \sum_{\substack{\text{3-valent} \\ \text{vertices } \alpha = 1}}^{4g+2s+n-4} \sum_{i=1}^{3 \bmod 3} \left(\frac{\partial f}{\partial Z_{\alpha_i}}\frac{\partial g}{\partial Z_{\alpha_{i+1}}} - \frac{\partial g}{\partial Z_{\alpha_i}}\frac{\partial f}{\partial Z_{\alpha_{i+1}}}\right), \tag{3.9}$$

where Z_α are the shear coordinates on each edge and the sum ranges all three-valent vertices of a graph and α_i are the labels of the cyclically (clockwise) ordered ($\alpha_4 \equiv \alpha_1$) edges incident to the vertex with the label α.

This bracket gives rise to the *Goldman bracket* on the space of geodesic length functions [20] and in [11] it is proved that on the lengths of the elements of a complete cusped geodesic lamination which consists only of arcs and simple loops this Poisson bracket gives rise to the cluster algebra Poisson structure.

In order to describe this Poisson structure more explicitly, notice that for cusped fat-graph with the additional property that the polygons containing holes with no cusps are monogons, every hole with no associated bordered cusps is contained inside a closed loop, which is an edge starting and terminating at the same three-valent vertex. Vice versa, every such closed loop corresponds to a hole with no associated bordered cusps. Therefore every open edge corresponding to a bordered cusp "protrudes" towards the interior of some face of the graph, and we have exactly one hole contained inside this face.

As a consequence of these facts, we can fix an orientation of the fat graph and of each open edge which allows us to determine a natural partition of the set of bordered cusps into nonintersecting (maybe empty) subsets δ_k, $k = 1, \ldots, s$ of cusps incident to the corresponding holes, and to set a cyclic ordering in every such subset. This means that all arcs in the lamination are uniquely determined by 4 indices, telling us in which cusp they originate and terminate and in what order they enter or exit the cusp. For example, if we orient the fat graph in Fig. 6 counterclockwise so that the arc d originates in cusp 2 and is the first arc in that cusp, then it terminates in cusp 1 and it is the eight arc in that cusp (we count arcs starting from the side of open edge that goes into the fat-graph), we can denote $d = g_{2_1,1_8}$. Analogously $b = g_{1_3,1_4}$ and so on. The formula for the Poisson brackets is then completely combinatorial:

$$\{g_{s_i,t_j}, g_{p_r,q_l}\} = g_{s_i,t_j}g_{p_r,q_l}\frac{\epsilon_{i-r}\delta_{s,p} + \epsilon_{j-r}\delta_{t,p} + \epsilon_{i-l}\delta_{s,q} + \epsilon_{j-l}\delta_{t,q}}{4}, \tag{3.10}$$

where $\epsilon_k := \mathrm{sign}(k)$.

In [11] it is proved that the abstract bracket defined by (3.10) is indeed a Poisson bracket.

4 Decorated character variety

The classical character varieties are moduli spaces of monodromy data of regular or singular connections, which can be considered like representation spaces of the fundamental group of a Riemann surface. Goldman proved that they are endowed with a holomorphic symplectic structure [20].

It is well-known that so-called Stokes data should be added to the classical monodromy in the case of non-fuchsian irregular singularities. That is why we want to generalize the previous representation space description to define an appropriate generalisation of the classical (or "tame") character variety. Various descriptions of generalized character varieties as spaces of representations of a "wild fundamental groupoid" [34], "Stokes groupoid" [21] or as "fissions" varieties of Stokes representations associated with a complex reductive linear algebraic group [5]. We will discuss these results at the end of this section.

In this paper we propose a different notion of decorated character variety which is based on the combinatorial description of Teichmüller space explained in the previous section. Our construction is based on the fact that topologically speaking a Riemann surface $\Sigma_{g,s,n}$ with s holes, with n bordered cusps is equivalent to a Riemann surface $\tilde{\Sigma}_{g,s,n}$ of genus g, with s holes and n marked points $m_1,\dots,m_n$ on the boundaries.

We introduce *the fundamental groupoid of arcs* $\mathfrak{U}$ as the set of all directed paths $\gamma_{ij}:[0,1]\to\tilde{\Sigma}_{g,s,n}$ such that $\gamma_{ij}(0)=m_i$ and $\gamma_{ij}(1)=m_j$ modulo homotopy. The groupoid structure is dictated by the usual path–composition rules.

For each m_j, $j=1,\dots,n$, the isotopy group

$$\Pi_j=\{\gamma_{jj}|\gamma_{jj}:[0,1]\to\tilde{\Sigma}_{g,s,n},\ \gamma_{jj}(0)=m_j,\ \gamma_{jj}(1)=m_j\}/\{\text{homotopy}\}$$

is isomorphic to the usual fundamental group and $\Pi_j=\gamma_{ij}^{-1}\Pi_i\gamma_{ij}$ for any arc $\gamma_{ij}\in\mathfrak{U}$ such that $\gamma_{ij}(0)=m_i$ and $\gamma_{ij}(1)=m_j$.

Using the decoration at each cusp, we associate to each arc γ_{ij} a matrix $M_{ij}\in SL_2(\mathbb{R})$ as explained in the previous section, for example $M_{ij}=X(k_j)LX(z_n)R\cdots LX(z_1)RX(k_i)$. In order to associate a matrix in $SL_2(\mathbb{C})$, we complexify the coordinates $Z_i\in\mathbb{C}$ in all formulas. We define the decorated character variety[‡] as:

$$\mathrm{Hom}\left(\mathfrak{U},SL_2(\mathbb{C})\right)/_{\prod_{j=1}^n B_j}, \tag{4.11}$$

where B_j is the Borel unipotent subgroup in $SL_2(\mathbb{C})$ - we mod out by one Borel unipotent subgroup for each cusp - this is very natural as the elements in the Borel unipotent subgroup naturally preserve parabolic the choice of horocycles. As a consequence, we define the characters:

$$\begin{aligned}\mathrm{Tr}_K:\quad & SL_2(\mathbb{C})\to\mathbb{C}\\ & M\mapsto \mathrm{Tr}(MK),\qquad \text{where}\quad K=\begin{pmatrix}0&0\\-1&0\end{pmatrix}.\end{aligned}$$

The complex dimension of the decorated character variety is $6g-6+3s+2n$. Infact, let us fix a bordered cusp as base point c_0, we have $2g$ matrices for the usual A- and B-cycles starting and terminating at c_0, $s-1$ matrices corresponding to going around all holes except the one to which the cusp c_0 belongs, $n-1$ matrices corresponding to paths starting at c_0 and terminating at other cusps. Each matrix depends on three independent complex coordinates, giving $3(2g+s-1+n-1)$, by taking the quotient by $\prod_{j=1}^n B_j$ we obtain the final result.

Note that for arcs γ_{jj} which are born and die in the same cusp, the usual character is also defined. Geometrically speaking $\mathrm{Tr}_K(\gamma_{jj})$ is a function of the length of the arc which is born and dies in cusp j (to be precise it is the exponential of the singed half length of the portion of the arc outside the fixed horocycle around the j-th cusp), while $\mathrm{Tr}\,\gamma_{jj}$ is a function of the length (the double of the hyperbolic cosine of the half length) of the closed geodesic homotopic to it.

To equip the decorated character variety with a Poisson bracket, we extend Poisson brackets (3.9) to the complexified shear coordinates. For $Z_i,Z_j\in\mathbb{C}$ we postulate $\{Z_i,Z_j\}=\{\overline{Z}_i,\overline{Z}_j\}:=\{Z_i,Z_j\}_{\mathbb{R}}$ and $\{Z_i,\overline{Z}_j\}\equiv 0$ or, explicitly, $\{\Re Z_i,\Re Z_j\}=-\{\Im Z_i,\Im Z_j\}=\frac{1}{2}\{Z_i,Z_j\}_{\mathbb{R}}$, $\{\Re Z_i,\Im Z_j\}\equiv 0$ where we let $\{Z_i,Z_j\}_{\mathbb{R}}$ denote the (constant) Poisson bracket (3.9). All formulas for Poisson brackets between characters then remain valid irrespectively on whether we consider real or complexified generalized shear coordinates Z_i.

The representation space of the fundamental groupoid of arcs (4.11) (before modding out by the product of Borel unipotent subgroups) carries a quasi-Hamiltonian structure. Originally, in [2] and [1] it was shown that the moduli spaces of flat connections can be obtained by a finite-dimensional reduction procedure (rather than infinite dimensional reduction like in the classical Atiyah-Bott definition of symplectic structure) and are equipped with a quasi-Hamiltonian structure. This construction was generalized in [5] for the case of the moduli

[‡]The authors are grateful to A. Alexeev and P. Severa for their helpful remarks on the formulation of this definition.

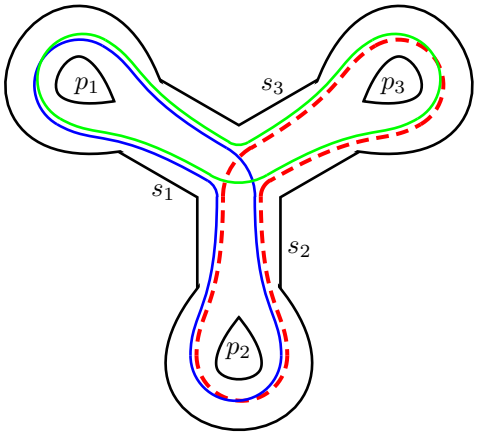

Fig. 4. The fat graph of the 4 holed Riemann sphere. The dashed geodesic is x_1; the solid geodesics are x_2 and x_3.

space of flat connections with irregular singularities and further by Li-Bland and Severa [29] who gave almost all necessary definitions to enlarge the quasi-Hamiltonian technic to the moduli space of connections on a surfaces with several marked points on its boundary components.

Our approach is very much in the spirit of the case of fundamental groupoid of "quilted varieties" (see [29]). We want to remind that in the case of four-holed sphere (PVI) the quasi-Hamiltonian structure on the representation space

$$\mathrm{Hom}\left(\pi_1(\mathbb{P}^1 \setminus \{0,t,1,\infty\}, SL_2(\mathbb{C})\right)$$

is given by the "Korotkin-Samtleben" quadratic brackets between matrix elements of the representation matrices which form a "not closed" Poisson algebra [28]. The Jacobi identity is satisfied only modding the conjugation [10]).

In our case the Poisson structure on the decorated character variety is an example of a "Trace-Poisson" quadratic structure of [30] and [4] defined on the representation space $\mathrm{Hom}\,(\mathfrak{U}, SL_2(\mathbb{C}))$ [12].

It is interesting to compare our approach to the one by Paul and Ramis who introduced the "wild fundamental groupoid" for PV [34]. Of course in our case, the construction is not restricted to PV, but covers all possible Riemann surfaces. Moreover our parametrisation has the advantage of making the confluence evident in terms of the Poisson structure.

In the next section we will provide a set of coordinates for the decorated character variety associated to each of the Riemann surfaces appearing in Fig. 3. These coordinates are the λ–lengths (or indeed the characters) of $6g-6+3s+2n$ arcs which form a lamination in the given Riemann surface:

Proposition 4.1. For any Riemann surface $\Sigma_{g,s,n}$ of genus g with s holes and $n \geq 1$ cusps there exists a complete lamination consisting of $6g-6+3s+2n$ arcs. □

This proposition was proved in [11] (see Prop. 4.1) . However, for convenience of the reader, in the next Section we will show in each case that the λ–lengths are indeed monomials in the exponentiated shear coordinates which are independent as proved [39] and [35].

5 Decorated character varieties and Painlevé monodromy manifolds

In the case of a Riemann sphere with 4 holes and no cusps, the fat graph is given in Fig. 4 and the three geodesics lengths x_1, x_2, x_3 of the three geodesics which go around two holes without self–intersections are enough to close the Poisson algebra.

By following the rules explained in Section 3, the following parameterisation of x_1, x_2, x_3 in shear coordinates on the fat-graph of a 4–holed sphere was found in [10]:

$$\begin{aligned}
x_1 &= -e^{s_2+s_3+\frac{p_2}{2}+\frac{p_3}{2}} - e^{-s_2-s_3-\frac{p_2}{2}-\frac{p_3}{2}} - e^{s_2-s_3+\frac{p_2}{2}-\frac{p_3}{2}} - G_2 e^{-s_3-\frac{p_3}{2}} - G_3 e^{s_2+\frac{p_2}{2}},\\
x_2 &= -e^{s_3+s_1+\frac{p_3}{2}+\frac{p_1}{2}} - e^{-s_3-s_1-\frac{p_3}{2}-\frac{p_1}{2}} - e^{s_3-s_1+\frac{p_3}{2}-\frac{p_1}{2}} - G_3 e^{-s_1-\frac{p_1}{2}} - G_1 e^{s_3+\frac{p_3}{2}},\\
x_3 &= -e^{s_1+s_2+\frac{p_1}{2}+\frac{p_2}{2}} - e^{-s_1-s_2-\frac{p_1}{2}-\frac{p_2}{2}} - e^{s_1-s_2+\frac{p_1}{2}-\frac{p_2}{2}} - G_1 e^{-s_2-\frac{p_2}{2}} - G_2 e^{s_1+\frac{p_1}{2}},
\end{aligned} \tag{5.12}$$

where

$$G_i = e^{\frac{p_i}{2}} + e^{-\frac{p_i}{2}}, \qquad i = 1, 2, 3,$$

and

$$G_\infty = e^{s_1+s_2+s_3+\frac{p_1}{2}+\frac{p_2}{2}+\frac{p_3}{2}} + e^{-s_1-s_2-s_3-\frac{p_1}{2}-\frac{p_3}{2}-\frac{p_3}{2}}.$$

Note that by complexifying $s_1, s_2, s_3, p_1, p_2, p_3$, we obtain a parameterisation of the PVI cubic, i.e. of the character variety of $SL_2(\mathbb{C})$ character variety of a Riemann sphere with 4 holes.

We are now going to produce a similar coordinate description of each of the other Painlevé cubics. We will provide a geometric description of the corresponding Riemann surface and its fat-graph and discuss the corresponding decorated character variety.

5.1 Decorated character variety for PV

The confluence from the cubic associated to PVI to the one associated to PV is realised by

$$p_3 \to p_3 - 2\log[\epsilon],$$

in the limit $\epsilon \to 0$. We obtain the following shear coordinate description for the PV cubic:

$$\begin{aligned}
x_1 &= -e^{s_2+s_3+\frac{p_2}{2}+\frac{p_3}{2}} - G_3 e^{s_2+\frac{p_2}{2}},\\
x_2 &= -e^{s_3+s_1+\frac{p_3}{2}+\frac{p_1}{2}} - e^{s_3-s_1+\frac{p_3}{2}-\frac{p_1}{2}} - G_3 e^{-s_1-\frac{p_1}{2}} - G_1 e^{s_3+\frac{p_3}{2}},\\
x_3 &= -e^{s_1+s_2+\frac{p_1}{2}+\frac{p_2}{2}} - e^{-s_1-s_2-\frac{p_1}{2}-\frac{p_2}{2}} - e^{s_1-s_2+\frac{p_1}{2}-\frac{p_2}{2}} - G_1 e^{-s_2-\frac{p_2}{2}} - G_2 e^{s_1+\frac{p_1}{2}},
\end{aligned} \tag{5.13}$$

where

$$G_i = e^{\frac{p_i}{2}} + e^{-\frac{p_i}{2}}, \quad i = 1, 2, \quad G_3 = e^{\frac{p_3}{2}}, \quad G_\infty = e^{s_1+s_2+s_3+\frac{p_1}{2}+\frac{p_2}{2}+\frac{p_3}{2}}.$$

These coordinates satisfy the following cubic relation:

$$\begin{aligned}
&x_1x_2x_3 + x_1^2 + x_2^2 - (G_1G_\infty + G_2G_3)x_1 - (G_2G_\infty + G_1G_3)x_2 -\\
&-G_3G_\infty x_3 + G_\infty^2 + G_3^2 + G_1G_2G_3G_\infty = 0.
\end{aligned} \tag{5.14}$$

Note that the parameter p_3 is now redundant, we can eliminate it by rescaling. To obtain the correct PV cubic, we need to pick $p_3 = -p_1 - p_2 - 2s_1 - 2s_2 - 2s_3$ so that $G_\infty = 1$.

Geometrically speaking, sending the perimeter p_3 to infinity means that we are performing a chewing-gum move: two holes, one of perimeter p_3 and the other of perimeter $s_1 + s_2 + s_3 + \frac{p_1}{2} + \frac{p_2}{2} + \frac{p_3}{2}$, become infinite, but the area between them remains finite, thus leading to a Riemann sphere with three holes and two cusps on one of them. In terms of the fat-graph, this is represented by Fig. 5.

The geodesic x_3 corresponds to the closed loop obtained going around p_1 and p_2, while x_1 and x_2 are arcs starting at one cusp, going around p_1 and p_2 respectively, and coming back to the other cusp.

As explained in Section 3, according to [11], the Poisson algebra related to the character variety of a Riemann sphere with three holes and two cusps on one boundary is 7-dimensional. The fat-graph admits a complete cusped lamination as displayed in Fig. 6 so that a full set of coordinates on the character variety is given by the complexification of the five elements in the lamination and of the two parameters G_1 and G_2 which determine the perimeter of the two non-cusped holes.

Remark 5.1. Observe that in the article [36] the cubic corresponding to the PV has exactly the same form as (5.14):

$$\begin{aligned}
C \;:=\; & d_1d_2d_3 + d_1^2 + d_2^2 - (s_1 + s_2s_3)d_1 - (s_2 + s_1s_3)d_2 -\\
& -s_3d_3 + 1 + s_3^2 + s_1s_2s_3 = 0,
\end{aligned} \tag{5.15}$$

The parameters s_i in (5.15) coincide with G_i in (5.14) for $i = 1, 2, 3$ (recall that $G_\infty = 1$), however the coordinates x_1, x_2, x_3 are quite different from d_1, d_2, d_3 in (5.15). Indeed the parameters d_i are the matrix elements of the triple of matrices (M_1, M_2, M_∞) which parametrise the differential system data in [36] and satisfy the condition $M_1M_2M_\infty = \mathbb{I}$. The matrix M_1 corresponds to our loop γ_b, M_2 corresponds to γ_a and M_∞ is given by the topological monodromy $\exp(2\pi i\Lambda S_1S_2)$ where $S_{1,2}$ are Stokes matrices and Λ is diagonal (the "formal monodromy"). Our x_1, x_2, x_3 instead are λ-lengths of certain arcs, for example $x_3 = \operatorname{Tr}_k(\gamma_e\gamma_b) \neq eb = \operatorname{Tr}_k e \operatorname{Tr}_k b$. To compare the triples d_i and x_i for $i = 1, 2, 3$ one should observe that both x_1, x_2, x_3 are d_1, d_2, d_3 are Laurent polynomials of our λ-lengths a, b, c, d, e so that indeed these is a bijection between these two sets of coordinates. This phenomenon presents itself for all other cubics and we won't repeat this discussion in each case. □

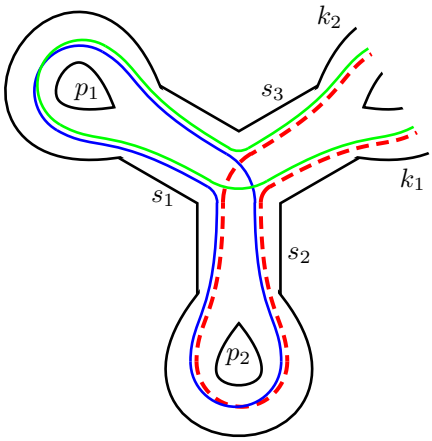

Fig. 5. The fat graph corresponding to PV. The geodesic x_3 remains closed, while x_1 (the dashed line) and x_2 become arcs.

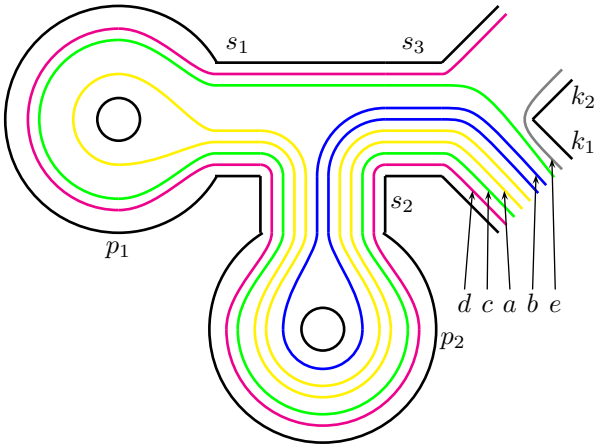

Fig. 6. The system of arcs for PV.

Remark 5.2. The family (5.15) appears in context of the Riemann-Hilbert fibraiton map and the corresponding affine coordinate rings admit the inclusion:

$$\mathbb{C}[s_1, s_2, s_3, s_3^{-1}] \hookrightarrow \mathbb{C}[d_1, d_2, d_3, s_1, s_2, s_3, s_3^{-1}]/(C).$$

This inclusion corresponds the projection of varieties:

$$\mathrm{Spec}(\mathbb{C}[d_1, d_2, d_3, s_1, s_2, s_3, s_3^{-1}]/(C)) \mapsto \mathrm{Spec}(\mathbb{C}[s_1, s_2, s_3, s_3^{-1}]).$$

This is a 5–dimensional fibration whose fibers over the 3–dimensional base $s_1, s_2, s_3 \in \mathbb{C} \times \mathbb{C} \times \mathbb{C}$ are singular cubic surfaces in $\mathbb{C}^3$, thus giving the PV–analogue of the fibrated family $\mathcal{S}(\bar{x}, \bar{\omega})$ described in the subsection 2.1. □

Notice that there are two shear coordinates associated to the two cusps, they are denoted by k_1 and k_2, their sum corresponds to what we call p_3 in (5.13). These shear coordinates do not commute with the other ones, they in fact satisfy the following relations:

$$\{s_3, k_1\} = \{k_1, k_2\} = \{k_2, s_3\} = 1.$$

As a consequence, the elements G_3 and G_∞ are not Casimirs in this Poisson algebra, despite being frozen variables in the cluster algebra setting (see Section 6)

In terms of shear coordinates, the elements in the lamination correspond to two loops (whose hyperbolic cosin length is denoted by G_1 and G_2 respectively) and five arcs whose lengths are expressed as follows:

$$\begin{aligned} a &= e^{k_1+s_1+2s_2+s_3+\frac{p_1}{2}+p_2}, \qquad b = e^{k_1+s_2+s_3+\frac{p_2}{2}}, \qquad e = e^{\frac{k_1}{2}+\frac{k_2}{2}}, \\ c &= e^{k_1+s_1+s_2+s_3+\frac{p_1}{2}+\frac{p_2}{2}}, \qquad d = e^{\frac{k_1}{2}+\frac{k_2}{2}+s_1+s_2+s_3+\frac{p_1}{2}+\frac{p_2}{2}}. \end{aligned} \tag{5.16}$$

They satisfy the following Poisson relations, which can be deduced by formula (3.10):

$$\begin{aligned}
&\{a,b\}=ab,\quad \{a,c\}=0,\quad \{a,d\}=-\frac{1}{2}ad,\quad \{a,e\}=\frac{1}{2}ae,\\
&\{b,c\}=0,\quad \{b,d\}=-\frac{1}{2}bd,\quad \{b,e\}=\frac{1}{2}be,\\
&\{c,d\}=-\frac{1}{2}cd,\quad \{c,e\}=\frac{1}{2}ce,\quad \{d,e\}=0,\quad \{G_1,\cdot\}=\{G_2,\cdot\}=0,
\end{aligned}\tag{5.17}$$

so that the elements G_1, G_2 and $G_3G_\infty = de$ are central.

The generic family of symplectic leaves are determined by the common level set of the three Casimirs G_1, G_2 and $G_3G_\infty = de$ and are 4-dimensional (rather than 2-dimensional like in the PVI case).

On each symplectic leaf, the PV monodromy manifold (5.14) is the subspace defined by those Laurent polynomials of a, b, c, d that depend polynomially on the Casimir values G_1, G_2, $G_3G_\infty = de$ which commute with the frozen variables, i.e. with $G_3 = e$ (and therefore with d as well, since de is a Casimir). To see this, we can use relations (5.16) to determine the exponentiated shear coordinates in terms of a, b, c, d, and then deduce the expressions of x_1, x_2, x_3 in terms of the lamination. We obtain the following expressions:

$$x_1 = -e\frac{a}{c} - d\frac{b}{c}, \qquad x_2 = -e\frac{b}{c} - G_1 d\frac{b}{a} - d\frac{b^2}{ac} - d\frac{c}{a},\tag{5.18}$$

$$x_3 = -G_2\frac{c}{b} - G_1\frac{c}{a} - \frac{b}{a} - \frac{c^2}{ab} - \frac{a}{b},\tag{5.19}$$

which automatically satisfy (5.14).

Due to the Poisson relations (5.17) the functions that commute with e are exactly the functions of $\frac{a}{b}, \frac{b}{c}, \frac{c}{a}, d$. Such functions may depend on the Casimir values G_1, G_2 and G_3G_∞ and e itself, so that $d = G_\infty$ becomes a parameter now. With this in mind, it is straightforward to prove that x_1, x_2, x_3 are algebraically independent functions of $\frac{a}{b}, \frac{b}{c}, \frac{c}{a}, d$ with polynomial coefficients in G_1, G_2, $G_3G_\infty = de$, so that x_1, x_2, x_3 form a basis in the space of functions which commute with e.

In similar fashion we can obtain also the character variety of PVI as a Poisson sub–algebra of the PV character variety defined by those Laurent polynomials of a, b, c, d that depend polynomially on the Casimir values G_1, G_2, and on $e + \frac{1}{e}$ (rather than polynomial in e like for the PV cubic) which commute with e. Setting:

$$\begin{aligned}
\tilde{x}_1 &= -(e+\frac{1}{e})\frac{a}{c} - d\frac{b}{c} - \frac{a^2}{bcd} - \frac{c}{bd} - G_2\frac{a}{bd},\\
\tilde{x}_2 &= -(e+\frac{1}{e})\frac{b}{c} - G_1 d\frac{b}{a} - d\frac{b^2}{ac} - d\frac{c}{a} - \frac{a}{cd},\\
\tilde{x}_3 &= -G_2\frac{c}{b} - G_1\frac{c}{a} - \frac{b}{a} - \frac{c^2}{ab} - \frac{a}{b},
\end{aligned}$$

we obtain exactly formulae (5.12) with the identification $x_i = \tilde{x}_i\big|_{k_1+k_3=p_3}$. This fact follows from the observation that $e^{\frac{p_3}{2}} + e^{-\frac{p_3}{2}}$ is the length function associated to the closed geodesic going around the third hole in PVI. This geodesic can be obtained as a concatenation of e with $\frac{1}{e}$ and the identification $k_1 + k_3 = p_3$.

5.2 Decorated character variety for PV_{deg}.

The confluence from PV to PV_{deg} is realised by the substitution

$$s_3 \to s_3 - \log[\epsilon],$$

in formulae (5.13). In the limit $\epsilon \to 0$ we obtain:

$$\begin{aligned}
x_1 &= -e^{s_2+s_3+\frac{p_2}{2}+\frac{p_3}{2}},\\
x_2 &= -e^{s_3+s_1+\frac{p_3}{2}+\frac{p_1}{2}} - e^{s_3-s_1+\frac{p_3}{2}-\frac{p_1}{2}} - G_1 e^{s_3+\frac{p_3}{2}},\\
x_3 &= -e^{s_1+s_2+\frac{p_1}{2}+\frac{p_2}{2}} - e^{-s_1-s_2-\frac{p_1}{2}-\frac{p_2}{2}} - e^{s_1-s_2+\frac{p_1}{2}-\frac{p_2}{2}} - G_1 e^{-s_2-\frac{p_2}{2}} - G_2 e^{s_1+\frac{p_1}{2}},
\end{aligned}\tag{5.20}$$

where

$$G_i = e^{\frac{p_i}{2}} + e^{-\frac{p_i}{2}}, \quad i = 1, 2, \quad G_\infty = e^{s_1+s_2+s_3+\frac{p_1}{2}+\frac{p_2}{2}+\frac{p_3}{2}}.$$

These coordinates satisfy the following cubic relation:

$$x_1x_2x_3 + x_1^2 + x_2^2 - G_1G_\infty x_1 - G_2G_\infty x_2 + G_\infty^2 = 0. \tag{5.21}$$

Note that the parameter p_3 is now redundant, we can eliminate it by rescaling. To obtain the correct PV_{deg} cubic, we need to pick $p_3 = -p_1 - p_2 - 2s_1 - 2s_2 - 2s_3$.

Geometrically speaking, sending the shear coordinate s_3 to infinity means that we are performing a cusp-removing move. In terms of the fat-graph, this is represented by Fig. 7.

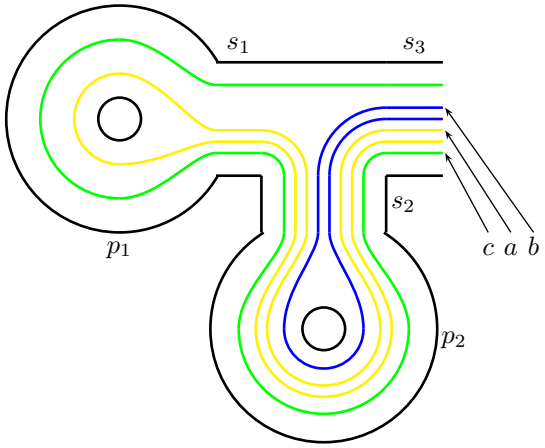

Fig. 7. The fat graph corresponding to PV_{deg} with the related system of arcs.

The character variety of a Riemann sphere with three holes and one cusp on one boundary is 5-dimensional. The fat-graph admits a complete cusped lamination so that a full set of coordinates on the character variety is given by the complexification of the geodesic length functions of the elements in the lamination. Now we have only one shear coordinate associated to the cusp, denoted by s_3, which does not commute with the other shear coordinates.

We omit the picture of the PV_{deg} lamination as it is very similar to Fig. 6, in which the edges labelled by k_1 and k_2 are removed and the geodesics d and e are lost.

In terms of shear coordinates, the elements in the lamination are two loops corresponding to the parameters G_1 and G_2 and three arcs for which the lengths are expressed as follows:

$$a = e^{s_1+2s_2+s_3+\frac{p_1}{2}+p_2}, \qquad b = e^{s_2+s_3+\frac{p_2}{2}}, \qquad c = e^{s_1+s_2+s_3+\frac{p_1}{2}+\frac{p_2}{2}}, \tag{5.22}$$

They satisfy the following Poisson relations, which can be deduced by formula (3.10):

$$\{a, b\} = ab, \quad \{a, c\} = 0, \quad \{b, c\} = 0, \quad \{G_1, \cdot\} = \{G_2, \cdot\} = 0, \tag{5.23}$$

so that the element c is a Casimir as well as the parameters G_1, G_2. Each symplectic leaf is two-dimensional and corresponds to the PV_{deg} monodromy manifold (5.21). Indeed, we can use relations (5.22) to determine the exponentiated shear coordinates in terms of a, b, c, and then deduce the expressions of x_1, x_2, x_3 in terms of the lamination. We obtain the following expressions:

$$x_1 = -b, \qquad x_2 = -G_1\frac{bc}{a} - \frac{b^2}{a} - \frac{c^2}{a}, \tag{5.24}$$

$$x_3 = -G_2\frac{c}{b} - G_1\frac{c}{a} - \frac{b}{a} - \frac{c^2}{ab} - \frac{a}{b}, \tag{5.25}$$

which automatically satisfy (5.21).

In terms of the lamination, the confluence from PV to PV_{deg} is given by the following prescription:

$$a \to a, \quad b \to b, \quad c \to c, \quad d \to 0, \quad e \to 0.$$

Note that the Poisson algebra (5.23) can be obtained as the Poisson sub-algebra of (5.17) defined by the functions of a, b, c only.

5.3 Decorated character variety for PIV

The confluence from the generic PV cubic (5.14) to the PIV one is realised by the substitution

$$p_2 \to p_2 - 2\log[\epsilon],$$

in formulae (5.13). In the limit $\epsilon \to 0$ we obtain:

$$\begin{aligned} x_1 &= -e^{s_2+s_3+\frac{p_2}{2}+\frac{p_3}{2}} - G_3 e^{s_2+\frac{p_2}{2}}, \\ x_2 &= -e^{s_3+s_1+\frac{p_3}{2}+\frac{p_1}{2}} - e^{s_3-s_1+\frac{p_3}{2}-\frac{p_1}{2}} - G_3 e^{-s_1-\frac{p_1}{2}} - G_1 e^{s_3+\frac{p_3}{2}}, \\ x_3 &= -e^{s_1+s_2+\frac{p_1}{2}+\frac{p_2}{2}} - G_2 e^{s_1+\frac{p_1}{2}}, \end{aligned} \tag{5.26}$$

where

$$G_1 = e^{\frac{p_1}{2}} + e^{-\frac{p_1}{2}}, \quad G_2 = e^{+\frac{p_2}{2}}, \quad G_3 = e^{+\frac{p_3}{2}}, \quad G_\infty = e^{s_1+s_2+s_3+\frac{p_1}{2}+\frac{p_2}{2}+\frac{p_3}{2}}.$$

These coordinates satisfy the following cubic relation:

$$\begin{aligned} &x_1x_2x_3 + x_1^2 - (G_1G_\infty + G_2G_3)x_1 - G_2G_\infty x_2 - \\ &-G_3G_\infty x_3 + G_\infty^2 + G_1G_2G_3G_\infty = 0. \end{aligned} \tag{5.27}$$

Note that the parameters p_3, p_2 are now redundant, we can eliminate it by rescaling. To obtain the correct PIV cubic, we need to pick $p_2 = p_3 = -p_1 - 2s_1 - 2s_2 - 2s_3$ so that $G_2 = G_3 = G_\infty$.

Similarly to the previous case, this means that we send the perimeter p_2 to infinity, which is a chewing-gum move leading to a Riemann sphere with two holes, one of which has 4 cusps on it. The corresponding fat-graph is given in Fig. 8, where we see 4 new shear coordinates, one for each cusp, so that in formulae (5.26) $p_2 = k_3 + k_4$ and $p_3 = k_1 + k_2$.

The character variety is now 8 dimensional and the complete cusped lamination is given in Fig. 8.

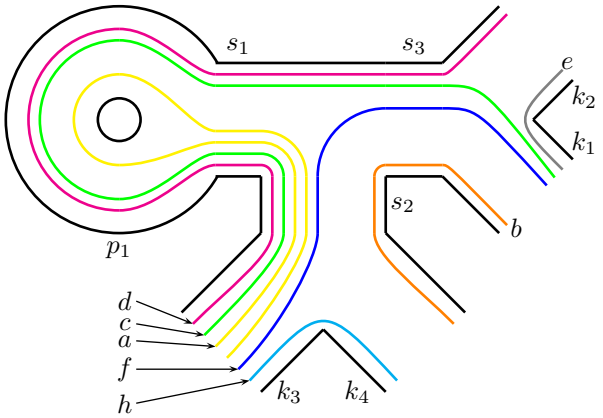

Fig. 8. The system of arcs for PIV.

In terms of shear coordinates, the elements in the lamination are expressed as follows:

$$\begin{aligned} &a = e^{s_1+s_2+k_3+\frac{p_1}{2}}, \quad b = e^{\frac{s_2}{2}+\frac{s_3}{2}+\frac{k_1}{2}+\frac{k_4}{2}}, \quad c = e^{s_1+\frac{s_2}{2}+\frac{s_3}{2}+\frac{p_1}{2}+\frac{k_1}{2}+\frac{k_3}{2}}, \\ &d = e^{s_1+\frac{s_2}{2}+\frac{s_3}{2}+\frac{p_1}{2}+\frac{k_2}{2}+\frac{k_3}{2}}, \quad e = e^{\frac{k_1}{2}+\frac{k_2}{2}}, \quad f = e^{\frac{s_2}{2}+\frac{s_3}{2}+\frac{k_1}{2}+\frac{k_3}{2}}, \quad h = e^{\frac{k_3}{2}+\frac{k_4}{2}}. \end{aligned} \tag{5.28}$$

The Poisson brackets can be easily extracted from (3.10):

$$\begin{aligned} &\{a,b\} = 0, \quad \{a,c\} = -\frac{1}{2}ac, \quad \{a,d\} = -\frac{1}{2}ad, \quad \{a,e\} = 0, \quad \{a,f\} = \frac{1}{2}af, \\ &\{a,h\} = \frac{1}{2}ah, \quad \{b,c\} = \frac{1}{4}bc, \quad \{b,d\} = 0, \quad \{b,e\} = \frac{1}{4}be, \quad \{b,f\} = \frac{1}{4}bf, \\ &\{b,h\} = -\frac{1}{4}bh, \quad \{c,d\} = -\frac{1}{4}cd, \quad \{c,e\} = \frac{1}{4}ce, \quad \{c,f\} = 0, \\ &\{c,h\} = \frac{1}{4}ch, \quad \{d,e\} = -\frac{1}{4}de, \quad \{d,f\} = \frac{1}{4}df, \quad \{d,h\} = \frac{1}{4}dh, \\ &\{e,f\} = -\frac{1}{4}ef, \quad \{e,h\} = 0, \quad \{f,h\} = \frac{1}{4}fh. \end{aligned} \tag{5.29}$$

The element $bdeh$ is a Casimir as well as the perimeter G_1. Each symplectic leaf is six-dimensional and the PIV monodromy manifold (5.27) is the subspace of those functions of $a, b, \ldots, h$ which commute with e and h. The proof of this statement is quite similar to the previously considered analogous assertion for the PV case and we omit it.

In terms of Poisson manifolds, the confluence from PV to PIV is *reversed*. Indeed the Poisson algebra (5.17) is a Poisson sub-algebra of (5.29) specified by the functions of

$$a_V := a_{IV} b_{IV}^2, \quad b_V := b_{IV} f_{IV}, \quad c_V := b_{IV} c_{IV}, \quad d_V := b_{IV} d_{IV},$$

where we have denoted with an index V the lamination coordinates in (5.17) and by IV the ones in (5.29). Note that h_{IV} is automatically a Casimir for the Poisson sub-algebra of (5.17) and can be identified with G_2.

5.4 Decorated character variety for $PIII^{D_6}$

The confluence from PV to $PIII^{D_6}$ is obtained by the following substitution:

$$s_1 \to s_1 + 2\log[\epsilon], \quad p_2 \to p_2 - 2\log[\epsilon], \quad p_1 \to p_1 - 2\log[\epsilon].$$

In the limit as $\epsilon \to 0$ we obtain:

$$\begin{aligned} x_1 &= -e^{s_2+s_3+\frac{p_2}{2}+\frac{p_3}{2}} - G_3 e^{s_2+\frac{p_2}{2}}, \\ x_2 &= -e^{s_3-s_1+\frac{p_3}{2}-\frac{p_1}{2}} - G_3 e^{-s_1-\frac{p_1}{2}} - G_1 e^{s_3+\frac{p_3}{2}}, \\ x_3 &= -e^{s_1+s_2+\frac{p_1}{2}+\frac{p_2}{2}} - e^{-s_1-s_2-\frac{p_1}{2}-\frac{p_2}{2}} - G_1 e^{-s_2-\frac{p_2}{2}} - G_2 e^{s_1+\frac{p_1}{2}}, \end{aligned} \tag{5.30}$$

where

$$\widetilde{G}_i = e^{\frac{p_i}{2}}, \quad i = 1,2,3 \quad \widetilde{G}_\infty = e^{s_1+s_2+s_3+\frac{p_1}{2}+\frac{p_2}{2}+\frac{p_3}{2}}.$$

These coordinates satisfy the following cubic relation:

$$x_1 x_2 x_3 + x_1^2 + x_2^2 - (\widetilde{G}_1\widetilde{G}_\infty + \widetilde{G}_2\widetilde{G}_3)x_1 - (\widetilde{G}_2\widetilde{G}_\infty + \widetilde{G}_1\widetilde{G}_3)x_2 + \widetilde{G}_1\widetilde{G}_2\widetilde{G}_3\widetilde{G}_\infty = 0. \tag{5.31}$$

We can pick $p_2 = p_3 = 0$ in order to obtain the correct $PIII^{D_6}$ cubic. Note that there is a slight discrepancy between the $\widetilde{G}_i$s in the cubic (5.31) and the G_is dictated by our formulae (2.4). This is easily solved by a simple transformation

$$G_\infty = \sqrt{\widetilde{G}_1\widetilde{G}_\infty}, \quad G_1 = \sqrt{\widetilde{G}_1\widetilde{G}_\infty} + \frac{1}{\sqrt{\widetilde{G}_1\widetilde{G}_\infty}}, \quad G_2 = \sqrt{\frac{\widetilde{G}_\infty}{\widetilde{G}_1}} + \sqrt{\frac{\widetilde{G}_1}{\widetilde{G}_\infty}}.$$

To understand the geometry of this confluence, we first need to flip the PV fat-graph to the equivalent graph given in Fig. 9.

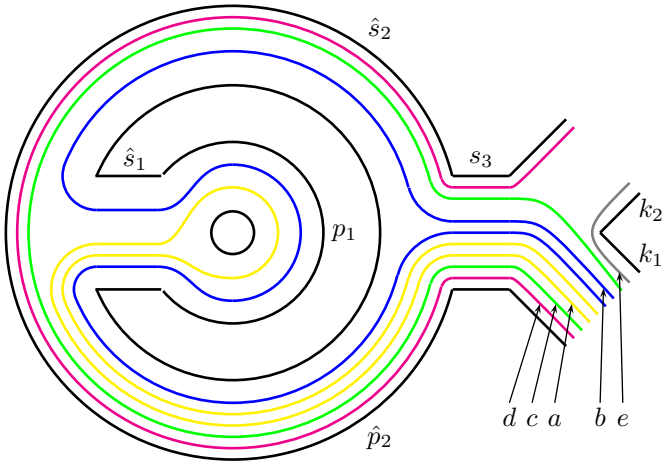

Fig. 9. Transformation of the PV system of arcs from Fig. 6 under a sequence of two flips.

The new shear coordinates are expressed in terms of the old ones as follows:

$$\begin{aligned}
\hat{s}_1 &= -s_1 - p_1 - \log(1+e^{s_2}),\\
\hat{s}_2 &= -s_2 + \log\left((1+e^{p_1+s_1}+e^{p_1+s_1+s_2})(1+e^{s_1}+e^{s_1+s_2})\right),\\
\hat{s}_3 &= s_3 - \log(1+e^{-s_2}), \quad \hat{p}_1 = p_1,\\
\hat{p}_2 &= p_2 + s_2 + p_1 + 2s_1 + 2\log(1+e^{s_2}) +\\
&+ \log\left((1+e^{p_1+s_1}+e^{p_1+s_1+s_2})(1+e^{s_1}+e^{s_1+s_2})\right).
\end{aligned} \tag{5.32}$$

Remark 5.3. Note that this flip is obtained by composing two mapping class group transformations described in Figures 3 and 4 of [11]. This means that the fat-graph of PV is mapped to an intermediate fat-graph which does not satisfy the property that the polygons containing holes with no cusps are monogons. This is not a problem as in fact we can map the lamination in Fig. 6 to this new fat-graph and then to Fig.9. □

In the new shear coordinates the substitution (5.30) becomes simply:

$$\hat{p}_1 \to \hat{p}_1 - 2\log[\epsilon],$$

which geometrically speaking corresponds to the fat-graph in Fig. 10, where we see 4 new shear coordinates, one for each cusp, so that $\hat{p}_2 = \hat{k}_3 + \hat{k}_4$ and $\hat{p}_1 = \hat{k}_5 + \hat{k}_6$. This is the fat-graph of a Riemann sphere with two holes each of them with two cusps.

Note that the coordinates in Fig. 10 are the true shear coordinates, namely they satisfy the Poisson brackets:

$$\begin{aligned}
&\{\hat{k}_2,\hat{s}_3\} = \{\hat{s}_3,\hat{k}_1\} = \{\hat{k}_1,\hat{k}_2\} = \{\hat{s}_3,\hat{s}_2\} = \{\hat{p}_2,\hat{s}_3\} = 1, \quad \{\hat{s}_2,\hat{p}_2\} = 2,\\
&\{\hat{s}_1,\hat{s}_2\} = \{\hat{p}_2,\hat{s}_1\} = \{\hat{s}_1,\hat{k}_5\} = \{\hat{k}_6,\hat{s}_1\} = \{\hat{k}_5,\hat{k}_6\} = 1,
\end{aligned} \tag{5.33}$$

If we use the limiting transformation of (5.32):

$$\begin{aligned}
\hat{s}_1 &= -s_1 - k_5 - k_6 - \log(1+e^{s_2}), \qquad \hat{s}_3 = s_3 - \log(1+e^{-s_2}),\\
\hat{s}_2 &= -s_2 + \log\left(1+e^{k_5+k_6+s_1}+e^{k_5+k_6+s_1+s_2}\right), \qquad \hat{p}_1 = p_1,\\
\hat{k}_1 &= k_1, \qquad \hat{k}_2 = k_2, \qquad \hat{k}_5 = k_5, \qquad \hat{k}_6 = k_6,\\
\hat{p}_2 &= p_2 + s_2 + k_5 + k_6 + 2s_1 + 2\log(1+e^{s_2}) +\\
&+ \log\left((1+e^{k_5+k_6+s_1}+e^{k_5+k_6+s_1+s_2})(1+e^{s_1}+e^{s_1+s_2}\right).
\end{aligned} \tag{5.34}$$

to go back to $s_1, s_2, s_3, p_2, k_1, k_2, k_5, k_6$, we see that k_5, k_6 have non standard Poisson brackets with s_1, s_2, s_3. This is due to the fact that this limiting transformation (5.34) destroys the geometry, as it essentially maps from a Riemann sphere with two holes each of them with two cusps to a Riemann sphere with two holes one of which has 4 cusps, and the other has no cusps (the PIV case). This implies that the correct coordinates to describe the character variety of a Riemann sphere with two holes each of them with two cusps are the complexified $\hat{s}_1, \hat{s}_2, \hat{s}_3, \hat{p}_2, \hat{k}_1, \hat{k}_2, \hat{k}_5, \hat{k}_6$.

This character variety is 8-dimensional. The fat-graph admits a complete cusped lamination as displayed in Fig. 10 so that a full set of coordinates on the character variety is given by the eight complexified elements in the lamination.

In terms of the shear coordinates $\hat{s}_1, \hat{s}_2, \hat{s}_3, \hat{p}_2, \hat{k}_1, \hat{k}_2, \hat{k}_5, \hat{k}_6$ the elements in the $PIII^{D_6}$ lamination are expressed as follows:

$$\begin{aligned}
&a = e^{\frac{\hat{k}_1+\hat{k}_6-\hat{s}_1+\hat{s}_3+\hat{p}_2}{2}} + e^{\frac{\hat{k}_1+\hat{k}_6+\hat{s}_1+\hat{s}_3+\hat{p}_2}{2}}, \qquad e = e^{\frac{\hat{k}_1+\hat{k}_2}{2}}, \qquad g = e^{\frac{\hat{k}_5+\hat{k}_6}{2}},\\
&b = e^{\frac{\hat{k}_1+\hat{k}_6-\hat{s}_1-\hat{s}_2+\hat{s}_3}{2}} + e^{\frac{\hat{k}_1+\hat{k}_6+\hat{s}_1-\hat{s}_2+\hat{s}_3}{2}} + e^{\frac{\hat{k}_1+\hat{k}_6+\hat{s}_1+\hat{s}_2+\hat{s}_3}{2}},\\
&c = e^{\frac{2\hat{k}_1+\hat{s}_2+2\hat{s}_3+\hat{p}_2}{2}}, \qquad d = e^{\frac{\hat{k}_1+\hat{k}_2+\hat{s}_2+2\hat{s}_3+\hat{p}_2}{2}},\\
&f = e^{\frac{\hat{k}_1+\hat{k}_5+\hat{s}_1+\hat{s}_3+\hat{p}_2}{2}}, \qquad h = e^{\frac{\hat{k}_5+\hat{k}_6+2\hat{s}_1+\hat{s}_2+\hat{p}_2}{2}}.
\end{aligned} \tag{5.35}$$

The Poisson brackets admit two Casimirs, de and hg so that the symplectic leaves are 6-dimensional. Within each symplectic leaf, the $PIII^{D_6}$ monodromy manifold is given by the set of functions which commute with d, e, g, h. To see this, we proceed in the same way as in the case of PV. On the monodromy manifold we set $e = \tilde{G}_3$, $d = \tilde{G}_\infty$, $h = \tilde{G}_2$ and $g = \tilde{G}_1$.

Note that, unlike the cases of PV (Fig. 6), PIV (Fig. 8), and PII (Fig. 15 below), the expressions for the λ-lengths of arcs in (5.35) are not monomials in the exponentiated shear coordinates. This is because, unlike the

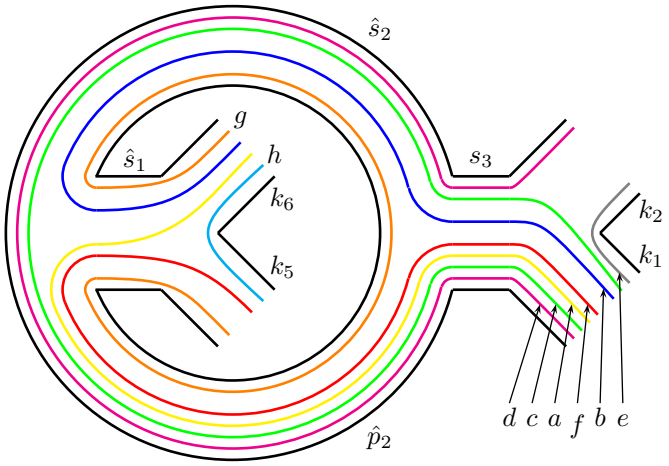

Fig. 10. The character variety for the $PIII$ system.

other named cases, the fat graph in Fig. 10 is not dual to the maximum cusped lamination $\{a,b,c,d,e,f,g,h\}$. We obtain the dual graph out of the one in Fig. 10 if we first flip the edge $\hat{s}_1$ subsequently flipping the edge $\hat{s}_2$. We depict the resulting fat graph and lamination in Fig. 11. In the transformed shear coordinates (indicated by tildes), the elements of the $PIII^{D_6}$ lamination read

$$\begin{aligned}
&a = e^{\frac{\tilde{k}_1+\tilde{k}_6+\tilde{s}_1+\tilde{s}_3+2\tilde{s}_2+\tilde{p}_2}{2}}, \qquad e = e^{\frac{\tilde{k}_1+\tilde{k}_2}{2}}, \qquad g = e^{\frac{\tilde{k}_5+\tilde{k}_6+\tilde{p}_2}{2}},\\
&b = e^{\frac{\tilde{k}_1+\tilde{k}_6+\tilde{s}_2+\tilde{s}_3}{2}}, \qquad c = e^{\frac{2\tilde{k}_1+\tilde{s}_1+\tilde{s}_2+2\tilde{s}_3+\tilde{p}_2}{2}}, \qquad d = e^{\frac{\tilde{k}_1+\tilde{k}_2+\tilde{s}_1+\tilde{s}_2+2\tilde{s}_3+\tilde{p}_2}{2}},\\
&f = e^{\frac{\tilde{k}_1+\tilde{k}_5+\tilde{s}_2+\tilde{s}_3+\tilde{p}_2}{2}}, \qquad h = e^{\frac{\tilde{k}_5+\tilde{k}_6+\tilde{s}_1+\tilde{s}_2}{2}}.
\end{aligned} \tag{5.36}$$

In this form, the homogeneity of the Poisson relations on the set $\{a,b,c,d,e,f,g,h\}$ becomes obvious:

$$\begin{aligned}
&\{a,b\} = \frac{1}{2}ab,\ \{a,c\} = 0,\ \{a,d\} = -\frac{1}{4}ad,\ \{a,e\} = \frac{1}{4}ae,\ \{a,f\} = \frac{1}{4}af,\\
&\{a,g\} = -\frac{1}{4}ag,\ \{a,h\} = \frac{1}{4}ah,\ \{b,c\} = 0,\ \{b,d\} = -\frac{1}{4}bd\,\{b,e\} = \frac{1}{4}be,\ \{b,f\} = -\frac{1}{4}bf,\\
&\{b,g\} = -\frac{1}{4}bg,\ \{b,h\} = \frac{1}{4}bh,\ \{c,d\} = -\frac{1}{2}cd,\ \{c,e\} = \frac{1}{2}ce,\ \{c,f\} = 0,\ \{c,g\} = 0,\\
&\{c,h\} = 0,\ \{d,e\} = 0,\ \{d,f\} = \frac{1}{4}df,\ \{d,g\} = 0,\ \{d,h\} = 0,\\
&\{e,f\} = -\frac{1}{4}ef,\ \{e,g\} = 0,\ \{e,h\} = 0,\ \{f,g\} = \frac{1}{4}fg,\ \{f,h\} = -\frac{1}{4}fh,\ \{h,g\} = 0.
\end{aligned} \tag{5.37}$$

It is interesting to construct the lamination and pattern in Fig. 10 as a limit of the corresponding system of PV. When we flip the fat-graph for PV, the lamination is flipped too as in Fig. 9.

When we open the inside hole to obtain the fat-graph for $PIII^{D_6}$, the PV arcs a and b break giving rise to the new arcs a, b and f and G_1 breaks up giving rise to g so that the confluence from PV to $PIII^{D_6}$ is again *reversed*. Indeed the Poisson algebra (5.17) is a Poisson sub-algebra of (5.37) specified by the functions of

$$a_V := a_{III} f_{III}, \quad b_V := b_{III} f_{III}, \quad c_V := c_{III}, \quad d_V := d_{III},$$

where we have denoted with an index V the lamination coordinates in (5.17) and by III the ones in (5.37). Note that h_{III} and g_{III} are automatically a Casimir for the Poisson sub-algebra of (5.17) and can be identified with G_2 and G_1 respectively.

5.5 Decorated character variety for $PIII^{D_7}$

The confluence from the generic $PIII^{D_6}$ cubic (5.31) to the $PIII^{D_7}$ one is realised by the substitution

$$s_3 \to s_3 - \log[\epsilon],$$

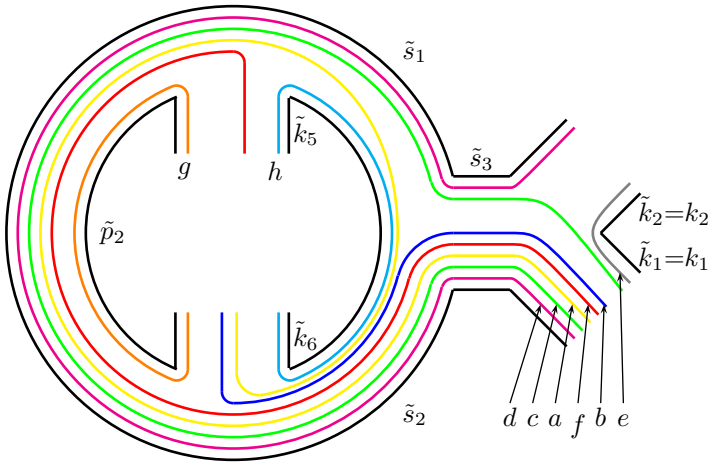

Fig. 11. The character variety for the $PIII$ system depicted on the fat graph dual to this variety.

in formulae (5.30). in the limit $\epsilon \to 0$ we obtain:

$$\begin{aligned} x_1 &= -e^{s_2+s_3+\frac{p_2}{2}+\frac{p_3}{2}}, \\ x_2 &= -e^{s_3-s_1+\frac{p_3}{2}-\frac{p_1}{2}} - G_1 e^{s_3+\frac{p_3}{2}}, \\ x_3 &= -e^{s_1+s_2+\frac{p_1}{2}+\frac{p_2}{2}} - e^{-s_1-s_2-\frac{p_1}{2}-\frac{p_2}{2}} - G_1 e^{-s_2-\frac{p_2}{2}} - G_2 e^{s_1+\frac{p_1}{2}}, \end{aligned} \tag{5.38}$$

where

$$G_i = e^{\frac{p_i}{2}}, \quad i = 1, 2, \quad G_3 = 0, \quad G_\infty = e^{s_1+s_2+s_3+\frac{p_1}{2}+\frac{p_2}{2}+\frac{p_3}{2}}.$$

These same expressions can equivalently obtained by the substitution:

$$s_1 \to s_1 + 2\log(\epsilon), \quad p_1 \to p_1 - 2\log(\epsilon), \qquad p_2 \to p_2 - 2\log(\epsilon),$$

in formulae (5.20) and by taking the limit as $\epsilon \to 0$.

These coordinates satisfy the following cubic relation:

$$x_1 x_2 x_3 + x_1^2 + x_2^2 - G_1 G_\infty x_1 - G_2 G_\infty x_2 = 0. \tag{5.39}$$

We can pick $p_2 = p_3 = 0$ and $s_3 = -s_1 - s_2 - \frac{p_1}{2}$ in order to obtain the correct $PIII^{D_7}$ cubic.

In terms of fat graph, we need to work with the coordinates (5.32), for which the confluence gives

$$\hat{s}_3 \to \hat{s}_3 - \log[\epsilon],$$

which corresponds to the fat-graph in Fig. 12. This corresponds to a Riemann sphere with two holes, one with one cusp and one with two cusps.

The character variety is 6 dimensional; the picture of the $PIII^{D_7}$ lamination is very similar to Fig. 10, in which the edges labelled by k_1 and k_2 are removed and the arcs d and e are lost. Again the Poisson brackets can be calculated using (3.10) and there are two Casimirs so that the symplectic leaves are 4 dimensional and that the Poisson algebra associated to $PIII^{D_7}$ is the Poisson sub-algebra of (5.37) given by the functions of a, b, c, f, g, h only. The $PIII^{D_7}$ monodromy manifold is given by those functions of a, b, c, d, f, h that commute with h.

5.6 Decorated character variety for $PIII^{D_8}$

The confluence from the generic $PIII^{D_7}$ cubic (5.39) to the $PIII^{D_8}$ one is realised by the substitution

$$s_1 \to s_1 + \log[\epsilon], \quad p_2 \to p_2 - 2\log[\epsilon]$$

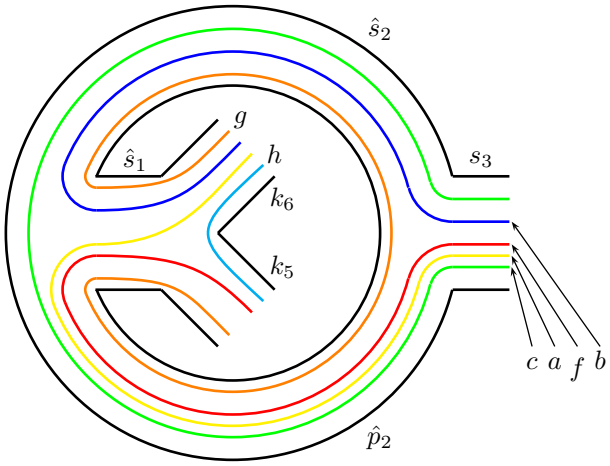

Fig. 12. The character variety of $PIII^{D_7}$.

in formulae (5.38). In the limit $\epsilon \to 0$ we obtain:

$$\begin{aligned} x_1 &= -e^{s_2+s_3+\frac{p_2}{2}+\frac{p_3}{2}}, \\ x_2 &= -e^{s_3-s_1+\frac{p_3}{2}-\frac{p_1}{2}}, \\ x_3 &= -e^{s_1+s_2+\frac{p_1}{2}+\frac{p_2}{2}} - e^{-s_1-s_2-\frac{p_1}{2}-\frac{p_2}{2}} - G_2 e^{s_1+\frac{p_1}{2}}, \end{aligned} \tag{5.40}$$

where

$$G_1 = 0, \quad G_2 = e^{\frac{p_2}{2}}, \quad i = 1, 2, \quad G_3 = 0, \quad G_\infty = e^{s_1+s_2+s_3+\frac{p_1}{2}+\frac{p_2}{2}+\frac{p_3}{2}}.$$

These coordinates satisfy the following cubic relation:

$$x_1 x_2 x_3 + x_1^2 + x_2^2 - G_2 G_\infty x_2 = 0. \tag{5.41}$$

We can pick $p_2 = p_3 = 0$ and $s_3 = -s_1 - s_2 - \frac{p_1}{2}$ in order to obtain the correct $PIII^{D_8}$ cubic.

In terms of fat graph, we need to work with the coordinates (5.32), for which the confluence gives

$$\hat{s}_1 \to \hat{s}_1 - \log[\epsilon],$$

which corresponds to the fat-graph in Fig. 13. This corresponds to a Riemann sphere with two holes, each with one cusp on it.

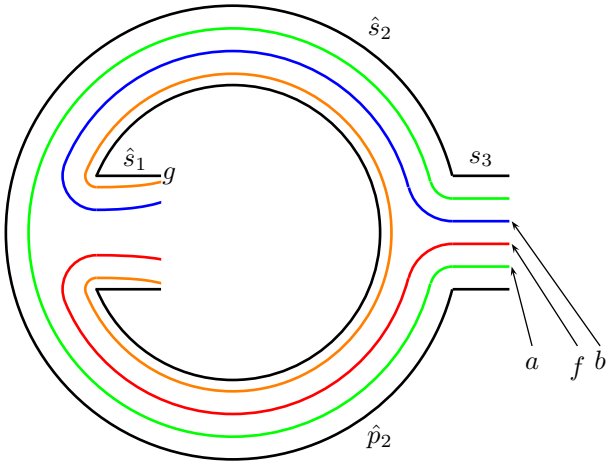

Fig. 13. The character variety of $PIII^{D_8}$.

The character variety is 4 dimensional and the Poisson brackets can be calculated using (3.10). and there are two Casimirs so that the symplectic leaves are 2 dimensional and coincide with the $PIII^{D_8}$ monodromy manifold. The Poisson algebra associated to $PIII^{D_8}$ is the Poisson sub-algebra of the one associated to $PIII^{D_7}$ given by the functions of a, b, c, h only.

5.7 Decorated character variety for PII^{JM}

The confluence from the generic PIV cubic (5.27) to the PII^{JM} cubic is realised by the substitution

$$p_1 \to p_1 - 2\log[\epsilon],$$

in formulae (5.26). In the limit $\epsilon \to 0$ we obtain:

$$\begin{aligned} x_1 &= -e^{s_2+s_3+\frac{p_2}{2}+\frac{p_3}{2}} - G_3 e^{s_2+\frac{p_2}{2}}, \\ x_2 &= -e^{s_3+s_1+\frac{p_3}{2}+\frac{p_1}{2}} - G_1 e^{s_3+\frac{p_3}{2}}, \\ x_3 &= -e^{s_1+s_2+\frac{p_1}{2}+\frac{p_2}{2}} - G_2 e^{s_1+\frac{p_1}{2}}, \end{aligned} \tag{5.42}$$

where

$$G_i = e^{\frac{p_i}{2}},\ i=1,2,3, \quad G_\infty = e^{s_1+s_2+s_3+\frac{p_1}{2}+\frac{p_2}{2}+\frac{p_3}{2}}.$$

These coordinates satisfy the following cubic relation:

$$\begin{aligned} &x_1x_2x_3 - G_1G_\infty x_1 - G_2G_\infty x_2 - \\ &-G_3G_\infty x_3 + G_\infty^2 + G_1G_2G_3G_\infty = 0. \end{aligned} \tag{5.43}$$

Note that the parameters p_3, p_2, p_1 are now redundant, we can eliminate it by rescaling. To obtain the correct PII^{JM} cubic, we need to pick $p_2 = p_3 = 0$ and $p_1 = -2s_1 - 2s_2 - 2s_3$.

Again, this means that we send the perimeter p_1 to infinity, which is a chewing-gum move leading to a Riemann sphere with one hole with 6 cusps on it. The corresponding fat-graph and corresponding lamination is given in Fig. 14 where we have 6 cusp shear coordinates $k_1, \dots, k_6$.

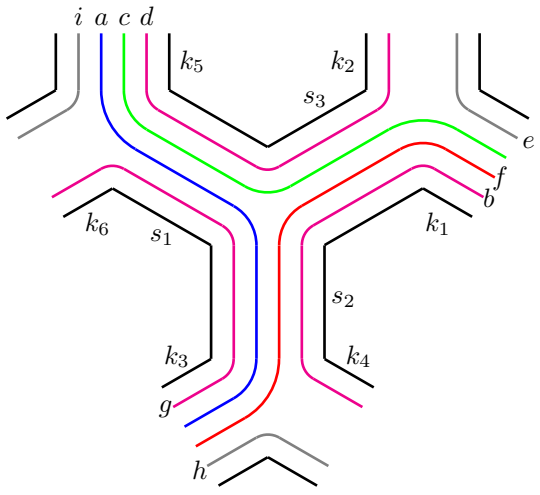

Fig. 14. The character variety of PII^{JM}.

The elements in the lamination read:

$$\begin{aligned} a = e^{\frac{s_1+s_2+k_3+k_5}{2}}, \quad b = e^{\frac{s_2+s_3+k_1+k_4}{2}}, \quad c = e^{\frac{s_1+s_3+k_1+k_5}{2}}, \quad d = e^{\frac{s_1+s_3+k_2+k_5}{2}}, \\ e = e^{\frac{k_1+k_2}{2}}, \quad f = e^{\frac{s_2+s_3+k_1+k_3}{2}}, \quad g = e^{\frac{s_1+s_2+k_3+k_6}{2}}, \quad h = e^{\frac{k_3+k_4}{2}}, \quad i = e^{\frac{k_5+k_6}{2}}. \end{aligned} \tag{5.44}$$

The character variety is now 9-dimensional, the Poisson brackets can be easily extracted from (3.10):

$$\begin{aligned}
&\{a,b\}=0,\quad \{a,c\}=-\frac{1}{4}ac,\quad \{a,d\}=-\frac{1}{4}ad,\quad \{a,e\}=0,\quad \{a,f\}=\frac{1}{4}af,\\
&\{a,g\}=-\frac{1}{4}ag,\quad \{a,h\}=\frac{1}{4}ah,\quad \{a,i\}=\frac{1}{4}ai,\quad \{b,c\}=\frac{1}{4}bc,\quad \{b,d\}=0,\\
&\{b,e\}=\frac{1}{4}be,\quad \{b,f\}=\frac{1}{4}bf,\quad \{b,g\}=0,\quad \{b,h\}=-\frac{1}{4}bh,\quad \{b,i\}=0,\\
&\{c,d\}=-\frac{1}{4}cd,\quad \{c,e\}=\frac{1}{4}ce,\quad \{c,f\}=-\frac{1}{4}cf,\quad \{c,g\}=0,\quad \{c,h\}=0,\\
&\{c,i\}=\frac{1}{4}ci,\quad \{d,e\}=-\frac{1}{4}de,\quad \{d,f\}=0,\quad \{d,g\}=0,\quad \{d,h\}=0,\\
&\{d,i\}=\frac{1}{4}di,\quad \{e,f\}=-\frac{1}{4}ef,\quad \{e,g\}=0,\quad \{e,h\}=0,\quad \{e,i\}=0,\\
&\{f,g\}=-\frac{1}{4}fg,\quad \{f,h\}=\frac{1}{4}fh\quad \{f,i\}=0,\quad \{g,h\}=\frac{1}{4}gh,\quad \{g,i\}=-\frac{1}{4}gi\quad \{h,i\}=0.
\end{aligned}\tag{5.45}$$

so that there is only one Casimir $bdeghi$. The confluence from the PIV character variety to the PII^{JM} one is again reversed, so that the Poisson algebra (5.29) is the sub-algebra of (5.45) defined by the functions of:

$$\begin{aligned}
&a_{IV}:=a_{II^{JM}}g_{II^{JM}},\quad b_{IV}:=b_{II^{JM}},\quad c_{IV}:=c_{II^{JM}}g_{II^{JM}},\quad d_{IV}:=d_{II^{JM}}g_{II^{JM}},\\
&e_{IV}:=e_{II^{JM}},\quad f_{IV}:=f_{II^{JM}},\quad h_{IV}:=h_{II^{JM}},
\end{aligned}$$

where we have indicated with an index IV the lamination coordinates associated to (5.29) and by an index II^{JM} the ones associated to (5.45).

Once again, let us stress that the PII^{JM} character variety (5.45) is the largest Poisson algebra appearing in the theory of the defferential Painlevé equations. This algebra corresponds to the triangulations of a hexagon ($3+6=9$ variables) which, for the Casimir value 1, is exactly the A_3 quiver in Sutherland's confluenced Dynkin diagrams [38].

The PII^{JM} monodromy manifold is given by the set of functions that Poisson commute with $p_1=k_5+k_6$, $p_2=k_3+k_4$ and $p_3=k_1+k_2$. We omit all details in this case.

5.8 Decorated character variety for PII^{FN}

The confluence from the generic PIV cubic (5.27) to the PII^{FN} cubic is realised by the substitution

$$s_3\to s_3-\log[\epsilon],$$

in formulae (5.26). In the limit $\epsilon\to 0$ we obtain:

$$\begin{aligned}
x_1 &= -e^{s_2+s_3+\frac{p_2}{2}+\frac{p_3}{2}},\\
x_2 &= -e^{s_3+s_1+\frac{p_3}{2}+\frac{p_1}{2}}-e^{s_3-s_1+\frac{p_3}{2}-\frac{p_1}{2}}-G_1e^{s_3+\frac{p_3}{2}},\\
x_3 &= -e^{s_1+s_2+\frac{p_1}{2}+\frac{p_2}{2}}-G_2e^{s_1+\frac{p_1}{2}},
\end{aligned}$$

where

$$G_1=e^{\frac{p_1}{2}}+e^{-\frac{p_1}{2}},\quad G_2=e^{\frac{p_2}{2}},\quad G_3=0,\quad G_\infty=e^{s_1+s_2+s_3+\frac{p_1}{2}+\frac{p_2}{2}+\frac{p_3}{2}}..$$

They satisfy the following cubic relation

$$x_1x_2x_3+x_1^2-G_1G_\infty x_1-G_2G_\infty x_2+G_\infty^2=0.\tag{5.46}$$

Observe that we can obtain exactly the same formulae by starting from the generic PV_{deg} cubic (5.21) by the substitution

$$p_2\to p_2-2\log[\epsilon],$$

and by taking the limit as $\epsilon\to 0$.

To obtain the PII^{FN} cubic we pick $p_2=p_3=0$ and $p_1=-2s_1-2s_2-2s_3$.

Geometrically speaking, sending the shear coordinate s_3 to infinity means that we are performing a cusp-removing move. This gives a Riemann sphere with two holes, one of them having three cusps on its boundary.

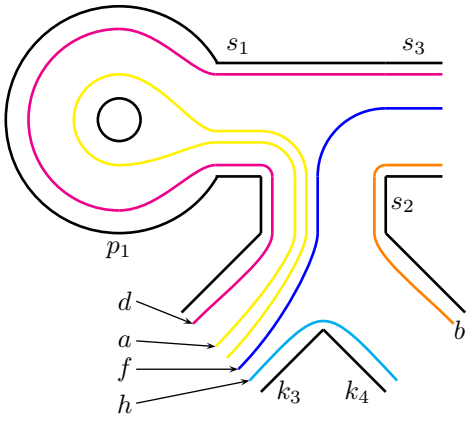

Fig. 15. The system of arcs for $PII^{\rm FN}$.

In terms of the fat-graph, this is represented by Fig. 15, where we wee three cusps of coordinates k_3, k_4 and s_3, so that in formulae (5.46) we must set $p_2 = k_3 + k_4$. .

The decorated character variety in this case is 6 dimensional. The lamination is given by the loop around the un-cusped-hole and the five arcs in Fig. 15.

The lengths of the arcs are

$$\begin{aligned} &a = e^{s_1+s_2+k_3+\frac{p_1}{2}}, \quad b = e^{\frac{s_2}{2}+\frac{s_3}{2}+\frac{k_4}{2}}, \\ &d = e^{s_1+\frac{s_2}{2}+\frac{s_3}{2}+\frac{p_1}{2}+\frac{k_3}{2}}, \quad f = e^{\frac{s_2}{2}+\frac{s_3}{2}+\frac{k_3}{2}}, \quad g = e^{\frac{k_3}{2}+\frac{k_4}{2}}. \end{aligned} \tag{5.47}$$

To show that our decorated character variety is not the same as the wild character variety (see [6] for the PII^{FN} case), we deal with this case in all details. The Poisson brackets among the complexified lamination arcs lengths are given by

$$\begin{aligned} &\{a,b\} = \{d,f\} = 0, \quad \{a,d\} = -\frac{ad}{2}, \quad \{a,f\} = \frac{af}{2}, \quad \{a,h\} = \frac{af}{2}, \\ &\{b,d\} = \frac{bd}{4}, \quad \{b,f\} = \frac{bf}{4}, \quad \{b,h\} = -\frac{bh}{4}, \quad \{d,h\} = \frac{dh}{4}, \quad \{f,h\} = \frac{fh}{4}. \end{aligned}$$

It is a straightforward computation to check that this is the Poisson sub-algebra of (5.29) given by the functions that do not depend on c and e and that there are two Casimirs, G_1 and bdh, so that the symplectic leaves are 4-dimensional. The PII^{FN} monodromy manifold (5.46) is the subspace of those functions of a, b, d, f, h which commute with h. To check that x_1, x_2 and x_3 commute with h it is enough to express them in terms of the lamination:

$$x_1 = -bf, \quad x_2 = -G_1\frac{df}{a} - \frac{d^2}{a} - \frac{f^2}{a}, \quad x_3 = -\frac{dh}{f} - \frac{ab}{f}.$$

Vice versa all functions commuting with h must have the form $a^\alpha b^\beta d^\delta f^\phi$ where $\alpha, \beta, \gamma, \delta, \phi$ are some numbers satisfying $2\alpha - \beta + \delta + \phi = 0$. Using this fact, it follows that on each symplectic leaf the set of functions which commute with h is 2-dimensional.

5.9 Decorated character variety for PI

The confluence from the generic PII^{JM} cubic to the PI one is realised by

$$s_3 \to s_3 - \log[\epsilon],$$

in formulae (5.42). In the limit $\epsilon \to 0$ we obtain:

$$\begin{aligned} x_1 &= -e^{s_2+s_3+\frac{p_2}{2}+\frac{p_3}{2}}, \\ x_2 &= -e^{s_3+s_1+\frac{p_3}{2}+\frac{p_1}{2}} - G_1 e^{s_3+\frac{p_3}{2}}, \\ x_3 &= -e^{s_1+s_2+\frac{p_1}{2}+\frac{p_2}{2}} - G_2 e^{s_1+\frac{p_1}{2}}, \end{aligned} \tag{5.48}$$

where

$$G_i = e^{\frac{p_i}{2}},\ i = 1, 2, \quad G_3 = 0, \quad G_\infty = e^{s_1+s_2+s_3+\frac{p_1}{2}+\frac{p_2}{2}+\frac{p_3}{2}}.$$

These coordinates satisfy the following cubic relation:

$$x_1x_2x_3 - G_1G_\infty x_1 - G_2G_\infty x_2 + G_\infty^2 = 0. \tag{5.49}$$

Observe that we can obtain exactly the same formulae by starting from the generic PII^{FN} cubic (5.46) in Flaschka-Newell form by the substitution

$$p_1 \to p_1 - 2\log[\epsilon],$$

and by taking the limit as $\epsilon \to 0$.

Note that the parameters p_3, p_2, p_1 and s_3 are now redundant, we can eliminate them by rescaling. We pick $p_1 = p_2 = p_3 = 0$ and $s_3 = -s_1 - s_2$, we obtain the correct PI by changing the sign of x_1 and x_2.

Geometrically speaking, sending the shear coordinate s_3 to infinity means that we are performing a cusp-removing move. In terms of the fat-graph, this is represented by Fig. 16.

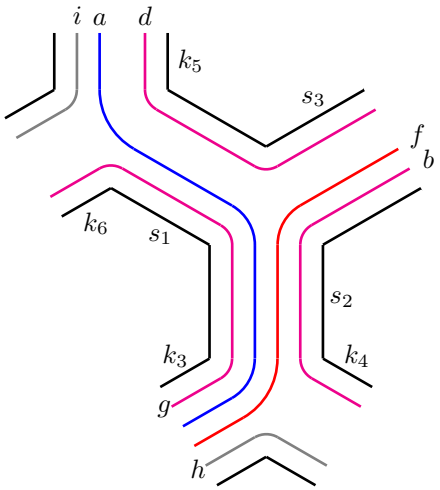

Fig. 16. The character variety of PI.

The character variety is now 7-dimensional, there is only one Casimir and the PI monodromy manifold is given by the set of functions that Poisson commute with $p_1 = k_5 + k_6$, $p_2 = k_3 + k_4$. We omit all details as they are similar to the previous cases.

5.10 Shear coordinates for the Weierstrass equation and Airy equation

5.10.1 *Weierstrass equation*

We now remove one further cusp from the generic PI cubic by replacing

$$s_1 \to s_1 - \log[\epsilon],$$

in formulae (5.48). In the limit $\epsilon \to 0$ we obtain:

$$\begin{aligned} x_1 &= -e^{s_2+s_3+\frac{p_2}{2}+\frac{p_3}{2}}, \\ x_2 &= -e^{s_3+s_1+\frac{p_3}{2}+\frac{p_1}{2}}, \\ x_3 &= -e^{s_1+s_2+\frac{p_1}{2}+\frac{p_2}{2}} - G_2 e^{s_1+\frac{p_1}{2}}, \end{aligned} \tag{5.50}$$

where

$$G_2 = e^{\frac{p_2}{2}}, \quad G_1 = G_3 = 0, \quad G_\infty = e^{s_1+s_2+s_3+\frac{p_1}{2}+\frac{p_2}{2}+\frac{p_3}{2}}.$$

These coordinates satisfy the following cubic relation:

$$x_1x_2x_3 - G_2G_\infty x_2 + G_\infty^2 = 0. \tag{5.51}$$

Note that the parameters p_3, p_2, p_1 and s_3 are now redundant, we can choose $p_1 = p_2 = p_3 = 0$ and $s_3 = -s_1 - s_2$ so that $G_2 = G_\infty = 1$. This gives us the following cubic

$$x_1 x_2 x_3 - x_2 + 1 = 0. \tag{5.52}$$

In order to relate this cubic to the Weiestrass elliptic curve, we need to projectivise it first:

$$x_1 x_2 x_3 - x_2 x_0^2 + x_0^3 = 0. \tag{5.53}$$

This cubic is now invariant under the following transformation

$$x_0 \to \alpha x_0, \quad x_1 \to \beta x_1, \quad x_2 \to \alpha x_2, \quad x_3 \to \frac{\alpha^2}{\beta} x_3,$$

so that we can rescale $x_2 \to 1$ and $x_3 \to x_1$, leading to the Weiestrass elliptic curve:

$$x_1^2 - x_0^2 + x_0^3 = 0.$$

The character variety in this case is a disk with 4 cusps. A lamination can be produced along the same lines as before.

5.10.2 *Airy equation*

If we remove one further cusp we obtain the character variety of a disk with 3 cusps. This corresponds to the famous Airy equation which the simplest linear ODE for which the Stokes phenomenon appears:

$$\frac{\mathrm{d}^2\psi}{\mathrm{d}z^2} + z\psi = 0, \quad \text{or in system form:} \quad \left(\frac{\mathrm{d}}{\mathrm{d}z} + \begin{pmatrix} 0 & -1 \\ z & 0 \end{pmatrix}\right) \begin{pmatrix} \psi \\ \psi' \end{pmatrix} = 0.$$

6 Painlevé cluster algebras: braid-group and affine MCG actions

6.1 Painlevé VI: analytic continuation and cluster mutations

In [15, 31] it was proved that the procedure of analytic continuation of a local solution to the sixth Painlevé equation corresponds to the following action of the braid group on the monodromy manifold:

$$\beta_1: \begin{array}{lcl} x_1 & \to & -x_1 - x_2 x_3 + \omega_1, \\ x_2 & \to & x_3, \\ x_3 & \to & x_2, \end{array} \tag{6.54}$$

$$\beta_2: \begin{array}{lcl} x_1 & \to & x_3, \\ x_2 & \to & -x_2 - x_1 x_3 + \omega_2, \\ x_3 & \to & x_1, \end{array} \tag{6.55}$$

$$\beta_3: \begin{array}{lcl} x_1 & \to & x_2, \\ x_2 & \to & x_1, \\ x_3 & \to & -x_3 - x_1 x_2 + \omega_3. \end{array} \tag{6.56}$$

In [10] it was shown that flips on the shear coordinates correspond to the action of the braid group on the cubic. The flips f_1, f_2, f_3 of the shear coordinates which give rise to the braid transformations $\beta_1\beta_2$ and β_3 respectively have the following form

$$f_1: \begin{array}{lcl} s_1 & \to & -p_1 - s_1, \qquad p_2 \to p_3, \qquad p_3 \to p_2, \\ s_2 & \to & s_3 + \log\left[1 + e^{s_1}\right] + \log\left[1 + e^{s_1 + p_1}\right], \\ s_3 & \to & s_2 - \log\left[1 + e^{-s_1}\right] + \log\left[1 + e^{-s_1 - p_1}\right], \end{array} \tag{6.57}$$

$$f_2: \begin{array}{lcl} s_1 & \to & s_3 - \log\left[1 + e^{-s_2}\right] - \log\left[1 + e^{-s_2 - p_2}\right], \\ s_2 & \to & -p_2 - s_2, \qquad p_1 \to p_3, \qquad p_3 \to p_1, \\ s_3 & \to & s_1 + \log\left[1 + e^{s_2}\right] + \log\left[1 + e^{s_2 + p_2}\right], \end{array} \tag{6.58}$$

$$f_3: \begin{array}{lcl} s_1 & \to & s_2 + \log\left[1 + e^{s_3}\right] + \log\left[1 + e^{s_3 + p_3}\right], \\ s_2 & \to & s_1 - \log\left[1 + e^{-s_3}\right] - \log\left[1 + e^{-s_3 - p_3}\right], \\ s_3 & \to & -p_3 - s_3 \qquad p_1 \to p_2, \qquad p_2 \to p_1. \end{array} \tag{6.59}$$

Remark 6.1. Observe that in [14] it was proved that shear coordinate flips (6.57), (6.58), (6.59) are indeed *dual* to the generalized cluster mutations (6.62) for the corresponding λ-lengths. □

We are now going to show that when $G_\infty = 2$ (geometrically this means that we have a puncture at infinity), the action of the braid group coincides with a *generalized cluster algebra structure* [14].

In order to see this let us compose each braid with a Okamoto symmetry in order to obtain the following

$$\widetilde{\beta}_i : \begin{array}{lcll} x_i & \to & -x_i - x_j x_k + \omega_i, & j,k \neq i, \\ x_j & \to & x_j, \quad \text{for} & j \neq i \end{array} \tag{6.60}$$

By using (2.2) this transformation acquires a cluster flavour:

$$\widetilde{\beta}_i : \; x_i x_i' = x_j^2 + x_k^2 + \omega_j x_j + \omega_k x_k + \omega_4 \quad j,k \neq i. \tag{6.61}$$

Indeed let us introduce the shifted variables:

$$y_i := x_i - G_i, \quad i = 1,2,3,$$

they satisfy the *generalized cluster algebra relation:*

$$\mu_i : \; y_i y_i' = y_j^2 + y_k^2 + G_i y_j y_k \quad j,k \neq i. \tag{6.62}$$

Note that generalized cluster algebras satisfy the Laurent phenomenon. In particular this result implies that procedure of analytic continuation of the solutions to the sixth Painlevé equation satisfies the Laurent phenomenon: if we start from a local solution corresponding to the point (y_1^0, y_2^0, y_3^0) on the shifted Painlevé cubic

$$y_1 y_2 y_3 + y_1^2 + y_2^2 + y_3^2 + G_1 y_2 y_3 + G_2 y_1 y_3 + G_3 y_1 y_2 = 0$$

any other branch of that solution will corresponds to points (y_1, y_2, y_3) on the same cubic such that each y_i is a Laurent polynomial of the initial (y_1^0, y_2^0, y_3^0).

6.2 Generalized cluster algebra structure for PV and $PV_{\mathbf{deg}}$

In this case, we have a Riemann surface $\Sigma_{0,3,2}$ with two bordered cusps on one hole. The only nontrivial Dehn twist is around the closed geodesic γ encircling these two holes (this geodesic is unique) – see the left side of Fig.18 here below.

We now consider the effect of this MCG transformation on the system of arcs in Fig. 6.

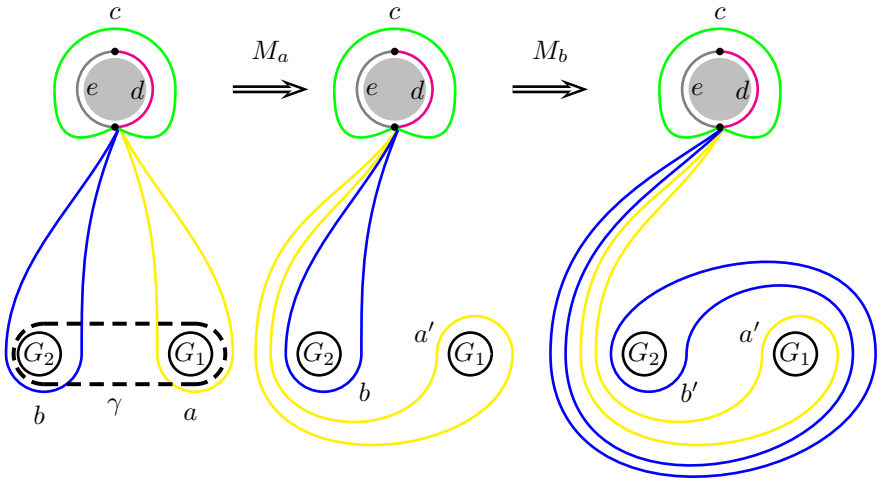

Fig. 17. The Dehn twist corresponding to γ maps the arcs in the left-hand side of this picture to those on the right-hand side. It is obtained by composing two generalized mutations M_a and M_b.

The generalized mutations M_a and M_b are given by the formulas

$$a'a = b^2 + c^2 + G_1 bc; \qquad b'b = (a')^2 + c^2 + G_2 a'c,$$

or, explicitly,

$$\begin{bmatrix} a \\ b \end{bmatrix} \to \begin{bmatrix} \dfrac{b^2+c^2+G_1bc}{a} \\ \dfrac{(b^2+c^2+G_1bc)^2}{a^2b} + G_2c\dfrac{b^2+c^2+G_1bc}{ba} + \dfrac{c^2}{b} \end{bmatrix}. \tag{6.63}$$

The geodesic function of γ is

$$G_\gamma = G_2\frac{c}{b} + G_1\frac{c}{a} + \frac{a}{b} + \frac{b}{a} + \frac{c^2}{ab} \tag{6.64}$$

and this function is the so-called *Hamiltonian MCG invariant:* it is the only MCG-invariant that generates the corresponding Dehn twist (see [27]), has nontrivial Poisson brackets with a and b, and is preserved by the MCG action (6.63).

In the case of $PV_{\rm deg}$, all the above formulas remain valid provided we replace c by the λ-length d of the boundary arc.

6.3 Generalized cluster algebra structure for $PIII^{D_6}$, $PIII^{D_7}$, and $PIII^{D_8}$

In all cases of $PIII^{D_6}$, we have a Riemann surface $\Sigma_{0,2,n}$ with $n_1 > 0$ and $n_2 > 0$, $n_1 + n_2 = n$, bordered cusps on the respective holes. For any n_1 and n_2, the only nontrivial Dehn twist is around the closed geodesic γ separating the holes (this geodesic is unique). Its geodesic function G_γ is the Hamiltonian MCG invariant. Besides this invariant, we have (non-Hamiltonian) invariants, which are λ-lengths of all arcs starting and terminating at the same boundary component.

We begin with the case of $PIII^{D_6}$ and consider the MCG action on the system of arcs in Fig. 10:

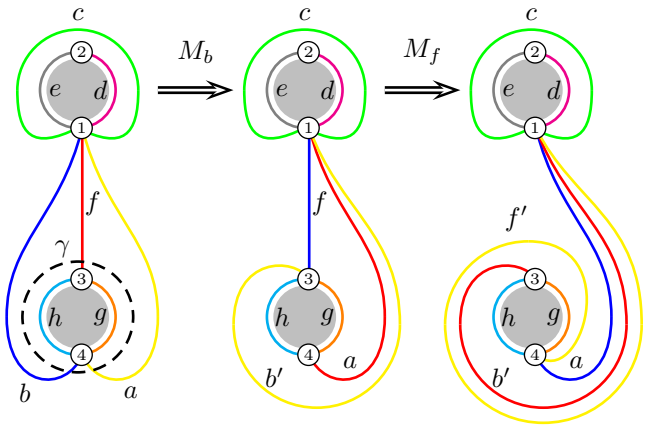

Fig. 18. The Dehn twist corresponding to γ maps the arcs in the left-hand side of this picture to those on the right-hand side. It is obtained by composing two generalized mutations M_b and M_f.

These transformations are governed by the standard mutation rules,

$$bb' = hc + fa, \qquad ff' = gc + ab';$$

in order to describe them in a more regular way, let us introduce the notation: we let $\lambda^{(i)}_{\alpha,\beta}$ denote the λ-length of the arc that goes between bordered cusps α and β (belonging to different boundary components) winding i times around the lower hole. For example,

$$f = \lambda^{(0)}_{1,3}, \quad b = \lambda^{(0)}_{1,4}, \quad a = \lambda^{(1)}_{1,4}, \quad b' = \lambda^{(1)}_{1,3}, \quad f' = \lambda^{(2)}_{1,4}, \quad c = \lambda_{1,1} \text{ etc.}$$

Note that $\lambda_{\alpha,\beta}$ with the labels α and β pertaining to the same boundary component are unique and invariant under the MCG action.

The net result of the Dehn twist on the triple $\{\lambda^{(i-1)}_{1,4}, \lambda^{(i-1)}_{1,3}, \lambda^{(i)}_{1,4}\}$ reads:

$$\begin{bmatrix} \lambda^{(i-1)}_{1,4} \\ \lambda^{(i-1)}_{1,3} \\ \lambda^{(i)}_{1,4} \end{bmatrix} \to \begin{bmatrix} \lambda^{(i)}_{1,4} \\ \dfrac{\lambda^{(i-1)}_{1,3}\lambda^{(i)}_{1,4} + h\lambda_{1,1}}{\lambda^{(i-1)}_{1,4}} \\ \dfrac{(\lambda^{(i)}_{1,4})^2}{\lambda^{(i-1)}_{1,4}} + \dfrac{h\lambda_{1,1}\lambda^{(i)}_{1,4}}{\lambda^{(i-1)}_{1,4}\lambda^{(i-1)}_{1,3}} + \dfrac{g\lambda_{1,1}}{\lambda^{(i-1)}_{1,3}} \end{bmatrix}. \tag{6.65}$$

This action admits two invariants: G_γ and $\lambda_{4,4}$ (the latter is obtained by the mutation of the element f, or $\lambda^{(i)}_{1,3}$):

$$G_\gamma = \frac{\lambda^{(i)}_{1,4}}{\lambda^{(i-1)}_{1,4}} + \frac{\lambda^{(i-1)}_{1,4}}{\lambda^{(i)}_{1,4}} + \frac{h\lambda_{1,1}}{\lambda^{(i-1)}_{1,3}\lambda^{(i-1)}_{1,4}} + \frac{g\lambda_{1,1}}{\lambda^{(i-1)}_{1,3}\lambda^{(i)}_{1,4}} \tag{6.66}$$

$$\lambda_{4,4} = \frac{g\lambda^{(i-1)}_{1,4}}{\lambda^{(i-1)}_{1,3}} + \frac{h\lambda^{(i)}_{1,4}}{\lambda^{(i-1)}_{1,3}} \tag{6.67}$$

The case of $PIII^{D_7}$ coincides with that of $PIII^{D_6}$, the geodesic $\lambda_{1,1}$ now becomes the boundary geodesic after erasing the bordered cusp 2.

In the case of $PIII^{D_8}$ we erase bordered cusps 2 and 3; the only MCG transformation is:

$$\begin{bmatrix} \lambda^{(i-1)}_{1,4} \\ \lambda^{(i)}_{1,4} \end{bmatrix} \to \begin{bmatrix} \lambda^{(i)}_{1,4} \\ \dfrac{(\lambda^{(i)}_{1,4})^2 + \lambda_{1,1}\lambda_{4,4}}{\lambda^{(i-1)}_{1,4}} \end{bmatrix}. \tag{6.68}$$

and the Hamiltonian MCG–invariant is

$$G_\gamma = \frac{\lambda^{(i)}_{1,4}}{\lambda^{(i-1)}_{1,4}} + \frac{\lambda^{(i-1)}_{1,4}}{\lambda^{(i)}_{1,4}} + \frac{\lambda_{1,1}\lambda_{4,4}}{\lambda^{(i-1)}_{1,4}\lambda^{(i)}_{1,4}}. \tag{6.69}$$

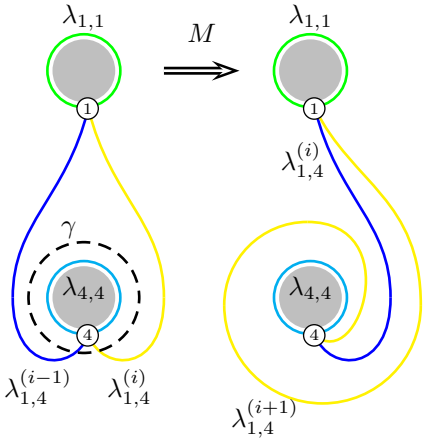

Fig. 19. The Dehn twist corresponding to γ maps the arcs in the left-hand side of this picture to those on the right-hand side and it is given by one generalized mutation M.

The cases of PIV, PII, and PI correspond to finite cluster algebras admitting no nontrivial modular transformations.

Appendix A Katz invariant and its geometric meaning

In this appendix we consider the Painlevé monodromy manifolds as moduli spaces of flat connections on $\mathbb{P} \setminus S$, where S is a set of isolated singularities ($S = \{0, 1, t, \infty\}$ for PVI, $S = \{0, 1, \infty\}$ for $PV, PIII^{D_6}$, $S = \{0, \infty\}$ for PIV, $S = \{\infty\}$ for PII and PI). Points in this singular locus S may be regular (for example in the case of PVI) or irregular. Irregular singular points are called "non-ramified" when the connection has non resonant residue at those points or "ramified" when the residue is resonant.

These moduli spaces have complex dimension 2 and are classified by the so-called *Katz invariants* associated to the singular locus S of the flat connection. Informally speaking, let z be the coordinate in the punctured Riemann sphere and denote by z_i the elements of S, then one can consider our flat connection as a local system whose local sections $q(z)$ have the following form:

$$q(z) = a_1(z - z_i)^{-k-1} + \dots a_k(z - z_i)^{-1}, \qquad \text{non-ramified case,}$$
$$q(z) = (z - z_i)^{\frac{1}{2}}[a_1(z - z_i)^{-k-\frac{1}{2}} + \dots a_*(z - z_i)^{-1}], \qquad \text{ramified case}$$

The number k is called Katz invariant of the singular point z_i.

The simple poles have Katz invariant $k = 0$ so that the PVI linear differential system has the Katz invariants $(0, 0, 0, 0)$. The confluence leads to two types of irregualr singularities: non-ramified with $k \in \mathbb{Z}$ and ramified ones with $k \in \frac{1}{2} + \mathbb{Z}$. For example the PV linear system has two simple poles $(0, 1)$ and the non-resonant irregular point ∞ with $k = 1$, so the Katz invariants are $(0, 0, 1)$, while the system for PI has one ramified singular point ∞ with $k = \frac{5}{2}$. See the precise definition of k and all computational details can be found in ([36]).

Our important observation is that the Katz invariants are given by the number of cusps on the corresponding hole divided by 2. So for example, PVI corresponds to a Riemann sphere with 4 holes and no cusps, so we have 0 cusps on each hole, giving $(0, 0, 0, 0)$ for the Katz invariants. For PV, we have two holes with no cusps and one hole with 2 cusps on it, dividing by 2 we obtain the Katz invariants $(0, 0, 1)$. The complete classification of the Katz invariants and the corresponding numbers of cusps is reported in the first three columns of table 2.

Painlevé eqs	no. of cusps	Katz invariants	no. Stokes rays	pole–orders for ϕ
PVI	$(0, 0, 0, 0)$	$(0, 0, 0, 0)$	$(0, 0, 0, 0)$	$(2, 2, 2, 2)$
PV	$(0, 0, 2)$	$(0, 0, 1)$	$(0, 0, 2)$	$(2, 2, 4)$
PV_{deg}	$(0, 0, 1)$	$(0, 0, 1/2)$	$(0, 0, 1)$	$(2, 2, 3)$
PIV	$(0, 4)$	$(0, 2)$	$(0, 4)$	$(2, 6)$
$PIII^{D_6}$	$(0, 2, 2)$	$(0, 1, 1)$	$(0, 2, 2)$	$(2, 4, 4)$
$PIII^{D_7}$	$(0, 1, 2)$	$(0, 1/2, 1)$	$(0, 1, 2)$	$(2, 3, 4)$
$PIII^{D_8}$	$(0, 1, 1)$	$(0, 1/2, 1/2)$	$(0, 1, 1)$	$(2, 3, 3)$
PII^{FN}	$(0, 3)$	$(0, 3/2)$	$(0, 3)$	$(2, 5)$
PII^{MJ}	6	3	6	8
PI	5	5/2	5	7

Table 2. For each Painlvé isomonodromic problem, this table displays the number of cusps on each hole for the corresponding Riemann surface, the Katz invariants associated to the corresponding flat connection, the number of Stokes rays in the linear system defined by the flat connection and the number of poles of the quadratic differential ϕ defined by the linear system.

As a consequence of this observation, our cusps indeed correspond to Stokes rays at the irregular singular points. Indeed in [36] $2k$ Stokes rays are attached to each singular point with Katz invariant k. Moreover this relation between the number of cusps and the Katz invariant fits well with the computation of orders of poles for the corresponding quadratic differential (= Hitchin systems) in the work by Gaiotto, Moore and Neitzke [19] : if the linear differential system for each isomonodromy problem has the form $\frac{dY}{dz} = A(z)Y$ then the corresponding quadratic differential is given by $\varphi(z) = \det A(z) dz^{\otimes 2}$. This means that our decorated character variety relates to the analytic properties of the quadratic differential φ: the number of the poles of φ defines the number of holes and the order of a φ pole minus 2 defines the number of cusps on the corresponding hole. If the matrix $A(z)$ has a pole of order n with diagonalisable leading residue matrix then the φ has a pole of order $2n$. If the residue leading matrix is non–diagonalisable then the quadratic differential has a pole of order $2n - 1$. For example, for $PIII^{D_8}$ there are double poles in 0 and in ∞ for $A(z)$, both have non–diagonalisable leading residue matrix. Hence, φ has two third order poles in these points and the corresponding monodromy surface is $\mathbb{P}^1$ with two holes and each of them has $3 - 2 = 1$ bordered cusps. The matrix $A(z)$ for PI has one pole of order 4, the quadratic differential has one pole with order $7 = 2 \times 4 - 1$ and the surface has $7 - 2 = 5$ cusps on the one hole (see table 2). Note that these results agree with the work by T. Sutherland [38] who used the auxiliary linear problem to produce a quadratic differential with high order poles on a punctured Riemann sphere. In his work, Sutherland associated a quiver to each of the above Painlevé cusped Riemann spheres and explicitly exhibit the canonical connected component of the space of numerical stability conditions of the Painlevé quivers.

Appendix B Singularity theory approach to the Painlevé cubics

As mentioned above, for special values of $\omega_1^{(d)}, \dots, \omega_4^{(d)}$ the fibre may have a singularity. Such singularities were classified in [24] for PVI and in [36] for all other Painlevé equations. These results can be summarised in the following table:

The meaning of the table is the following: for each Painlevé equation of type specified by the first column in the table, there is at least one singular fibre with singularity of the type given in the second column of the table, and at least one singular fibre with singularity of type specified by any Dynkin sub-diagram of the Dynkin

Painlevé equations	Surface singularity type
P_{VI}	D_4
P_V	A_3
deg P_V=$P_{III}(\tilde{D}_6)$	A_1
P_{III}	A_1
$P_{III}^{\tilde{D}_7}$	non-singular
$P_{III}^{\tilde{D}_8}$	non-singular
P_{IV}	A_2
P_{II}^{FN}	A_1
P_{II}^{MJ}	A_1
P_I	non-singular

Table 3.

diagram given in the second column of the table. For example PIV has a two singular fibres with singularity of type A_2 and at three singular fibres with singularity of type A_1.

The scope of this section is to show that the non singular fibres of each family of affine cubics are locally diffeomorphic to the versal unfolding [3] of the singularity of the type given in the second column of the table.

B.4 PVI

The cubic in this case is:

$$x_1x_2x_3 + x_1^2 + x_2^2 + x_3^2 + \omega_1x_1 + \omega_2x_2 + \omega_3x_3 + \omega_4 = 0. \tag{B.1}$$

To show that this is diffeomorphic to the versal unfolding of the D_4 we need to map this cubic to Arnol'd form. To this aim we first shift all variables by $x_i \to x_i + 2$, $i = 1, 2, 3$ to obtain

$$x_1^2 + x_2^2 + x_3^2 + 2x_1x_2 + 2x_2x_3 + 2x_1x_3 + x_1x_2x_3 + \widetilde{\omega}_1x_1 + \widetilde{\omega}_2x_2 + \widetilde{\omega}_3x_3 + \widetilde{\omega}_4 = 0, \tag{B.2}$$

where

$$\widetilde{\omega}_i = \omega_i + 8, \quad \text{for } i = 1, 2, 3, \qquad \widetilde{\omega}_4 = \omega_4 + 2(\omega_1 + \omega_2 + \omega_3) + 20.$$

As a second step we use the following diffeomorphism around the origin:

$$x \to x - \frac{1}{2}y, \quad y \to x + \frac{1}{2}x, \quad z \to z + \frac{y^2}{8} - 2x - \frac{x^2}{2} - \frac{\widetilde{\omega}_3}{2}$$

so that the new cubic (up to a Morse singularity that we throw away and after a shift $x \to x - \frac{\omega_3}{4}$) becomes indeed the versal unfolding of a D_4 singularity in Arnol'd form:

$$-2x_1^3 + \frac{x_1x_2^2}{2} + \widehat{\omega}_1x_1 + \widehat{\omega}_2x_2 + \widehat{\omega}_3x_1^2 + \widehat{\omega}_4,$$

where

$$\widehat{\omega}_1 = \omega_1 + \omega_2 - 8 - 4\omega_3 - \frac{\omega_3^2}{8}, \quad \widehat{\omega}_2 = \frac{\omega_2 - \omega_1}{2},$$
$$\widehat{\omega}_3 = 8 + \omega_3, \quad \widehat{\omega}_4 = \omega_4 + 2\omega_3 - \frac{\omega_3(\omega_1 + \omega_2 - \omega_3)}{4} + 4.$$

The above formulae show that the versal unfolding parameters $\widehat{\omega}_1, \ldots, \widehat{\omega}_4$ are independent as long as $\omega_1, \ldots, \omega_4$ are.

B.5 PV

The cubic in this case is:

$$x_1x_2x_3 + x_1^2 + x_2^2 + \omega_1x_1 + \omega_2x_2 + \omega_3x_3 + \omega_4 = 0, \tag{B.3}$$

where only three parameters are free:

$$\omega_1 = -G_2G_3 - G_1, \quad \omega_2 = -G_1G_3 - G_2, \quad \omega_3 = -G_3, \quad \omega_4 = 1 + G_3^2 + G_1G_2G_3.$$

Again we want to show that this is diffeomorphic to the versal unfolding of A_3. To this aim we impose the following change of variables:

$$x_1 \to u(x_2), \quad x_2 \to x_1 - x_3 + \frac{G_3}{u(x_2)}, \quad x_3 \to 2\frac{x_3}{u(x_2)} + \frac{G_2 + G_1G_3}{u(x_2)} - \frac{2G_3}{u(x_2)^2}, \tag{B.4}$$

where $u(x_2)$ is a function to be determined. This maps the PV cubic to:

$$x_1^2 - x_3^2 + 1 + G_1G_2G_3 + G_3^2 + \frac{G_3^2}{u^2} - \frac{G_3(G_2 + G_1G_3)}{u} - (G_1 + G_2G_3)u + u^2.$$

It is easy to prove that any solution $u(x_2)$ of the equation

$$\frac{G_3^2}{u^2} - \frac{G_3(G_2 + G_1G_3)}{u} - (G_1 + G_2G_3)u + u^2 = x_2^4 + (G_2 + G_1G_3)x_2^2 + (G_1 + G_2G_3)x_2$$

will define a diffeomorphism by (B.4) mapping (B.3) to the versal unfolding of A_3.

B.6 PIV

The cubic in this case is:

$$x_1x_2x_3 + x_1^2 + \omega_1x_1 + \omega_2x_2 + \omega_3x_3 + \omega_4 = 0, \tag{B.5}$$

where only two parameters are free:

$$\omega_1 = -G_1G_\infty - G_\infty^2, \quad \omega_2 = -G_\infty^2, \quad \omega_3 = -G_\infty^2, \quad \omega_4 = G_\infty^2 + G_1G_\infty^3.$$

Again we want to show that this is diffeomorphic to the versal unfolding of A_2. To this aim we impose the following change of variables:

$$x_1 \to x_1 - x_3 + \frac{G_\infty^2}{u}, \quad x_2 \to u, \quad x_3 \to \frac{2x_3}{u} + \frac{G_\infty}{u}(G_1 + G_\infty) - \frac{2G_\infty^2}{u^2} \tag{B.6}$$

where u is function of x_3 satisfying the following

$$\frac{G_\infty^4}{u^2} - \frac{G_\infty^3(G_\infty + G_1)}{u} - G_\infty^2u = x_2^3 + G_\infty x_2.$$

It is easy to prove that this transformation is a local diffeomorphism mapping our cubic to

$$x_1^2 - x_3^2 + x_2^3 + G_\infty x_2 + G_\infty + G_1G_\infty^3,$$

the versal unfolding of the A_2 singularity.

B.7 $PIII^{D_6}$ and PV_{deg}

The two cubics for $PIII^{D_6}$ and PV_{deg} are equivalent. We choose to work with the PV_{deg} one:

$$x_1x_2x_3 + x_1^2 + x_2^2 + \omega_1x_1 + \omega_2x_2 + 1 = 0, \tag{B.7}$$

where only two parameters are free:

$$\omega_1 = -G_1, \quad \omega_2 = -G_2.$$

The most singular fibre is given by $G_1 = 2$ and $G_2 = 2$ and has two singular points at $(1, 0, 2)$ and $(0, 1, 2)$ respectively. We can define two local diffeomorphisms, one around $(1, 0, 2)$, the other around $(0, 1, 2)$, which map our cubic to the versal unfolding of a A_1 singularity.

The first diffeomorphism is given by:

$$x_1 \to x_1 - \frac{\omega_1}{2}, \quad x_2 \to -x_2 + x_3, \quad x_3 \to -\frac{2(2x_3 + \omega_2)}{2x_1 - \omega_1}$$

The second diffeomorphism is:

$$x_1 \to -x_1 + x_3, \quad x_2 \to -x_2 - \frac{\omega_2}{2}, \quad x_3 \to \frac{2(2x_3 + \omega_1)}{2x_2 + \omega_2}.$$

B.7.1 *PII*

The two PII cases are equivalent via a simple transformation (see Remark 2.1), so we choose to work with the Jimbo-Miwa case:

$$x_1x_2x_3 - x_1 - x_2 - x_3 + \omega_4 = 0, \tag{B.8}$$

where:

$$\omega_4 = 1 + G_1.$$

The following change of variables:

$$x_1 \to x_1 - x_3 + \frac{1}{u}, \quad x_2 \to u, \quad x_3 \to \frac{x_1 + x_3 + 1}{u},$$

where u is a function of x_2 satisfying

$$-\frac{1}{u} - u = x_2^2,$$

is a local diffeomorphism mapping our cubic to the versal unfolding of the A_1 singularity:

$$x_1^2 - x_3^2 + x_2^2 + \omega_4.$$

Acknowledgements

The authors are grateful to A. Alexeev, P. Clarkson, M. Kontsevich, O.Lisovyy, V.Pestun, P. Severa, Y. Soibelman and T. Sutherland for helpful discussions. We are thankful to B.V. Dang for his help with SINGULAR package and to the two referees for their insightful questions which have resulted in a much enhanced paper. The work of L.O.Ch. was partially supported by the center of excellence grant "Centre for Quantum Geometry of Moduli Spaces" from the Danish National Research Foundation (DNRF95) and by the Russian Foundation for Basic Research (Grant Nos. 14-01-00860-a and 13-01-12405-ofi-m2). This research was supported by the EPSRC Research Grant $EP/J007234/1$, by the Hausdorff Institute, by ANR "DIADEMS", by RFBR-12-01-00525-a, by RFBR-15-01-05990, MPIM (Bonn) and SISSA (Trieste).

References

[1] Alekseev, A., Kosmann-Schwarzbach, Y., Meinrenken E. "Quasi-Poisson manifolds." *Canad. J. Math.,* 54 no. 1 (2002): 3–29.
[2] Alekseev A., Malkin A., Meinrenken E., Lie group valued moment maps., *J. Differential Geom.,* **48** (1998), no. 3:445–495.
[3] Arnol'd V. I., Critical points of smooth functions and their normal forms, *Russian Math. Surveys,* **30** (1975), no.5:3–65.
[4] Avan J., Ragoucy E., Rubtsov V., Quantization and Dynamisation of Trace-Poisson Brackets, *Commun. Math. Phys.,* **341** (2016), no. 1:263–287.
[5] Boalch P., Geometry and braiding of Stokes data; fission and wild character varieties, *Ann. of Math. (2),* **179** (2014), no. 1:301–365.
[6] Boalch P., Wild Character Varieties, points on the Riemann sphere and Calabi's examples, *arXiv:1501.00930* (2015).
[7] Cantat S., Loray, F., Dynamics on character varieties and Malgrange irreducibility of Painlevé VI equation. *Ann. Inst. Fourier (Grenoble)* **59** (2009), no. 7:2927–2978.
[8] Chekhov L., Fock V., A quantum Techmüller space, *Theor. and Math. Phys.,* **120** (1999), 1245–1259.
[9] Chekhov L., Fock V., Quantum mapping class group, pentagon relation, and geodesics, *Proc. Steklov Math. Inst.,* **226** (1999), 149–163.
[10] Chekhov L., Mazzocco M., Shear coordinates on the versal unfolding of the D_4 singularity, *J. Phys. A. Math. Gen.,* **43**, (2010), 1–13.
[11] Chekhov L., Mazzocco M., Colliding holes in Riemann surfaces and quantum cluster algebras, *arXiv:1509.07044* (2015).
[12] Chekhov L., Mazzocco M., Rubtsov V., quantized Painleve monodromy manifolds and Calabi-Yau algebras, *in progress.*
[13] Chekhov L., Mazzocco M., Rubtsov V., Quantum Stokes Phenomenon, *in progress.*
[14] Chekhov L., Shapiro M., Teichmüller spaces of Riemann surfaces with orbifold points of arbitrary order and cluster variables, *Int. Math. Res. Not. IMRN,* **2014**, no. 10:2746–2772.
[15] Dubrovin B.A., Mazzocco M., Monodromy of certain Painlevé-VI transcendents and reflection group, *Invent. Math.* **141** (2000), 55–147.
[16] Flaschka H. and Newell A.C., Monodromy and spectrum preserving deformations I, *Commun. Math. Phys.***76** (1980) 65–116.
[17] Fock V.V., Combinatorial description of the moduli space of projective structures, http://arxiv.org/abs/hep-th/9312193hep-th/9312193.
[18] Fock V.V., Dual Teichmüller spaces, http://arxiv.org/abs/dg-ga/9702018dg-ga/9702018.
[19] Gaiotto D., Moore G. W., Neitzke A., Wall-crossing, Hitchin systems, and the WKB approximation, *Adv. Math.,* **234** (2013), 239–403.
[20] Goldman W.M., *Invariant functions on Lie groups and Hamiltonian flows of surface group representations*, *Invent. Math.* **85** (1986), 263–302.
[21] Gualtieri M., Li S., Pym B., The Stokes groupoids, *J. Reine Angew. Math.,* to appear in (2016)
[22] Gross M., Hacking P., Keel S., Mirror symmetry for log Calabi-Yau surfaces I, *Publ. Math. Inst. Hautes Études Sci.,***122** (2015), 65–168.
[23] Hitchin N., Frobenius manifolds (with notes by David Calderbank), *NATO Adv. Sci. Inst. Ser. C Math. Phys. Sci.,* **488** (1997) 69–112.

[24] Inaba M., Iwasaki K., Saito M., Dynamics of the sixth Painlevé equation, in *Théories asymptotiques et équations de Painlevé, Sémin. Congr.,* **14** (2006) 103–167.
[25] Jimbo M., Monodromy Problem and the Boundary Condition for Some Painlevé Equations, *Publ. RIMS, Kyoto Univ.,* **18** (1982) 1137–1161.
[26] Jimbo M. and Miwa T.,Monodromy preserving deformations of linear ordinary differential equations with rational coefficients II, *Physica 2D,* **2** (1981), no. 3, 407–448.
[27] Kashaev R. M., *On the spectrum of Dehn twists in quantum Teichmüller theory*, in: *Physics and Combinatorics*, (Nagoya 2000). River Edge, NJ, World Sci. Publ., 2001, 63–81; math.QA/0008148.
[28] Korotkin D. and Samtleben H., Quantization of coset space σ-models coupled to two-dimensional gravity, *Comm. Math. Phys.* **190** (1997), no. 2, 411–457.
[29] Li-Bland D., Severa P., Symplectic and Poisson geometry of the moduli spaces of flat connections over quilted surfaces. *http://xxx.lanl.gov/abs/1304.0737v.2*
[30] Massuyeau G., Turaev V., Quasi-Poisson structures on representation spaces of surfaces, *IMRN,* **2014** no1:1–64 (2014).
[31] Mazzocco M., Rational solutions of the Painleve' VI equation, Kowalevski Workshop on Mathematical Methods of Regular Dynamics (Leeds, 2000). *J. Phys. A* **34** (2001), no. 11, 2281–2294.
[32] Mazzocco M., Confluences of the Painlevé equations, Cherednik algebras and q-Askey scheme, *http://arxiv.org/abs/1307.6140* to appear on *Nonlinearity* (2016).
[33] Oblomkov A., Double Affine Hecke Algebras of Rank 1 and Affine Cubic Surfaces, *IMRN,* **2004** no.18:877–912.
[34] Paul E., Ramis, Jean-Pierre, Dynamics on Wild Character Varieties, *SIGMA* 11 (2015), 068, 21 pages
[35] Penner R.C., *The decorated Teichmüller space of Riemann surfaces*, *Comm. Math. Phys.* **113** (1988), 299–339.
[36] Saito M., van der Put M., Moduli spaces for linear differential equations and the Painlevé equations, *arXiv:0902.1/02v5* (2009).
[37] Sakai H., Rational Surfaces Associated with Affine Root Systems and Geometry of the Painlevé Equations, *Commun. Math. Phys.* **220**, (2001) 165–229.
[38] Sutherland T., PhD thesis, (2013).
[39] Thurston W. P., *Minimal stretch maps between hyperbolic surfaces*, preprint (1984), math.GT/9801039.